Title:
Oldest known marine turtle? A new protostegid from the Lower Cretaceous of Colombia

Journal Issue:
PaleoBios, 32(1)

Author:
Cadena, Edwin A, Centro de Investigaciones Paleontológicas
Parham, James F, John D. Cooper Archaeological and Paleontological Center, California State University, Fullerton, CA

Publication Date:
2015

Permalink:
http://escholarship.org/uc/item/147611bv

Acknowledgements:
Financial support for this project was provided by the following funding organizations: Palaeontological Association (research grant, 2012), Karl Hirsch Memorial Grant, Western Interior Paleontological Society (2012), the Doris O. and Samuel P. Welles Research Fund of the University of California Museum of Paleontology (2012), Paleontological Research Institution (2012), Chicago Herpetological Society (2012), Toomey Foundation for the Natural Sciences (2012), and the Alexander von Humboldt Foundation of Germany. We thank A. Krapf (NMW), P. Holroyd (UCMP), R. Ernst (MTKD), and V. Schneider (NCSM) for help with access to specimens. Special thanks to C. B. Padilla (R.I.P), S. Padilla, M. Parra and her brothers for their amazing job at the Center of Paleontological Investigations and for allowing us access to the specimens.

Author Bio:
Assistant Professor, Department of Geological Sciences

Keywords:
Testudines, South America, Sea turtles, Villa de Leyva, upper Barremian-lower Aptian

Local Identifier:
ucmp_paleobios_28615

Abstract:
Recent studies suggested that many fossil marine turtles might not be closely related to extant marine turtles (Chelonioidea). The uncertainty surrounding the origin and phylogenetic position of fossil marine turtles impacts our understanding of turtle evolution and complicates our attempts

to develop and justify fossil calibrations for molecular divergence dating. Here we present the description and phylogenetic analysis of a new fossil marine turtle from the Lower Cretaceous (upper Barremian-lower Aptian, >120 Ma) of Colombia that has a minimum age that is >25 million years older than the minimum age of the previously recognized oldest chelonioid. This new fossil taxon, *Desmatochelys padillai* sp. nov., is represented by a nearly complete skeleton, four additional skulls with articulated lower jaws, and two partial shells. The description of this new taxon provides an excellent opportunity to explore unresolved questions about the antiquity and content of Chelonioidea. We present an updated global character-taxon matrix that includes *D. padillai* and marine turtles known from relatively complete specimens. Our analysis supports *D. padillai* as sister taxon of *D. lowi* within Protostegidae, and places protostegids as the sister to Pan-*Dermochelys* within Chelonioidea. However, this hypothesis is complicated by discrepancies in the stratigraphic appearance of lineages as well as necessarily complicated biogeographic scenarios, so we consider the phylogeny of fossil marine turtles to be unresolved and do not recommend using *D. padillai* as a fossil calibration for Chelonioidea. We also explore the definition of “marine turtle,” as applied to fossil taxa, in light of many littoral or partially marine-adapted fossil and extant lineages. We conclude that whereas the term “oldest marine turtle” depends very much on the concept of the term being applied, we can confidently say that *D. padillai* is the oldest, definitive, fully marine turtle known to date.

Supporting material:

Cadena_Parham_NexusFileDesPadillai

PaleoBios 32:1–42, September, 2015

PaleoBios

OFFICIAL PUBLICATION OF THE UNIVERSITY OF CALIFORNIA MUSEUM OF PALEONTOLOGY

Edwin A. Cadena and James F. Parham (2015). Oldest known marine turtle? A new protostegid from the Lower Cretaceous of Colombia.

Cover illustration: *Desmatochelys padillai* on an early Cretaceous beach. Reconstruction by artist Jorge Blanco, Argentina.

Citation: Cadena, E.A. and J.F. Parham. 2015. Oldest known marine turtle? A new protostegid from the Lower Cretaceous of Colombia. *PaleoBios* 32. ucmp_paleobios_28615.

PaleoBios 32:1–42, September, 2015

Oldest known marine turtle? A new protostegid from the Lower Cretaceous of Colombia

EDWIN A. CADENA[1, 2*] AND JAMES F. PARHAM[3]

[1] Centro de Investigaciones Paleontológicas, Villa de Leyva, Colombia; cadenachelys@gmail.com.

[2] Department of Paleoherpetology, Senckenberg Naturmuseum, 60325 Frankfurt am Main, Germany.

[3] John D. Cooper Archaeological and Paleontological Center, Department of Geological Sciences, California State University, Fullerton, CA 92834, USA; jparham@fullerton.edu.

Recent studies suggested that many fossil marine turtles might not be closely related to extant marine turtles (Chelonioidea). The uncertainty surrounding the origin and phylogenetic position of fossil marine turtles impacts our understanding of turtle evolution and complicates our attempts to develop and justify fossil calibrations for molecular divergence dating. Here we present the description and phylogenetic analysis of a new fossil marine turtle from the Lower Cretaceous (upper Barremian-lower Aptian, >120 Ma) of Colombia that has a minimum age that is >25 million years older than the minimum age of the previously recognized oldest chelonioid. This new fossil taxon, *Desmatochelys padillai* sp. nov., is represented by a nearly complete skeleton, four additional skulls with articulated lower jaws, and two partial shells. The description of this new taxon provides an excellent opportunity to explore unresolved questions about the antiquity and content of Chelonioidea. We present an updated global character-taxon matrix that includes *D. padillai* and marine turtles known from relatively complete specimens. Our analysis supports *D. padillai* as sister taxon of *D. lowi* within Protostegidae, and places protostegids as the sister to Pan-*Dermochelys* within Chelonioidea. However, this hypothesis is complicated by discrepancies in the stratigraphic appearance of lineages as well as necessarily complicated biogeographic scenarios, so we consider the phylogeny of fossil marine turtles to be unresolved and do not recommend using *D. padillai* as a fossil calibration for Chelonioidea. We also explore the definition of "marine turtle," as applied to fossil taxa, in light of many littoral or partially marine-adapted fossil and extant lineages. We conclude that whereas the term "oldest marine turtle" depends very much on the concept of the term being applied, we can confidently say that *D. padillai* is the oldest, definitive, fully marine turtle known to date.

Keywords: Testudines, South America, Sea turtles, Villa de Leyva, upper Barremian-lower Aptian

INTRODUCTION

Fossil turtles are rare in the Triassic and Lower Jurassic, but are one of the most abundant vertebrate fossils from the Upper Jurassic onward (~160 Ma and younger rocks). The complete fossil record of turtles has led them to be used as an exemplar for studies of fossil calibrated divergence dating using molecular sequences (Near et al. 2005, Parham and Irmis 2008, Near et al. 2008, Marshall 2008, Dornburg et al. 2011, Joyce et al. 2013, Warnock et al. 2015) and allowed for other comparisons of fossil and molecular data (Crawford et al. 2015). The phylogenetic positions of many fossil turtles are poorly justified, leading to uncertain estimates for some of the key nodes of the turtle tree of life (Parham and Irmis 2008, Joyce et al. 2013, Warnock et al. 2015). One of the most problematic clades is Chelonioidea Oppel, 1811 the crown group of marine turtles (all phylogenetic definitions follow Joyce et al. 2004). In addition to extant species, Chelonioidea is traditionally considered to include most fossil cryptodires that show any morphological specializations for a marine ecology such as paddle-like limbs, cordiform shells, and salt glands (Hirayama 1998). Recently, however, some studies suggested that many of these fossil marine turtles might not be closely related to the extant marine turtles (Joyce 2007, Joyce et al. 2013, Rabi et al. 2013, Parham et al. 2014, Crawford et al. 2015). The uncertainty surrounding the origin and phylogenetic position of fossil marine turtles impacts our understanding of turtle evolution and complicates our attempts to develop and justify fossil calibrations for molecular divergence dating.

The focal taxon for the problems surrounding the antiquity of chelonioids is *Santanachelys gaffneyi* Hirayama, 1998 from the Lower Cretaceous (Aptian-Albian) of Brazil. *Santanachelys gaffneyi* is considered by some to be the oldest known marine turtle, and the oldest chelonioid (Near et al. 2005, Kear and Lee 2006, Lapparent de Broin et al. 2014a), and so has been used as a fossil calibration for Chelonioidea in some studies (Near et al. 2005, Marshall 2008, Dornburg et al. 2011). *Santanachelys gaffneyi* is a member of the clade

**author for correspondence*

Citation: Cadena, E.A. and J.F. Parham. 2015. Oldest known marine turtle? A new protostegid from the Lower Cretaceous of Colombia. *PaleoBios* 32. ucmp_paleobios_28615.

Permalink: http://escholarship.org/uc/item/147611bv

Protostegidae Cope, 1872, a clade of specialized marine turtles that radiated during the Early Cretaceous (besides protostegids, all other putative chelonioids first appear in the Late Cretaceous). A global phylogenetic analysis of fossil turtles (Joyce 2007) included six marine turtles, with *S. gaffneyi* as the sole representative of the Protostegidae. In contrast to all other analyses, Joyce (2007) placed *S. gaffneyi* far from the other taxa, raising the possibility that protostegids are not chelonioids, but rather represent an earlier, independent marine radiation. Other authors note that this pattern is more consistent with the timing and geography of major turtle lineages in the fossil record (Parham and Pyenson 2010, Joyce et al. 2013, Pyenson et al. 2014, Parham et al. 2014, Crawford et al. 2015).

Here we present the description and phylogenetic analysis of a new fossil marine turtle from the Lower Cretaceous of South America (Paja Formation, Colombia) (Etayo-Serna 1979, Patarroyo 2000, 2004, Hoedemaeker 2004). One of the specimens representing this new species has been previously figured and reported by Smith (1989), Nicholls (1992), and Elliott et al. (1997), and attributed to *Desmatochelys* Williston, 1894. However, it has never been properly described or included in a phylogenetic analysis. The minimum age of the new species (120.0 Ma.)(Cohen et al. 2013) is much older than the minimum possible age for *S. gaffneyi* (92.8 Ma, see Joyce et al. 2013) and so it provides an excellent opportunity to explore unresolved questions about the antiquity and content of Chelonioidea. Given the uncertain phylogenetic position of protostegids we will refer to the "traditional" grouping of marine turtles that includes protostegids, dermochelyids, and cheloniids as Chelonioidea *sensu lato*, a provisional, informal name. We will refer to the crown group chelonioids (*Dermochelys coriacea* [Vandellius, 1761] and Cheloniidae [Oppel, 1811]) as Chelonioidea following Joyce et al. (2004). Note that, depending on their phylogenetic position, protostegids may or may not be considered chelonioids, but by our provisional definition, will always be considered chelonioids *sensu lato*. Except where specified the phylogenetic nomenclature and terminology (e.g., pan prefix) follows Joyce et al. (2004).

MATERIALS AND METHODS

Specimens

Material of *Desmatochelys padillai* sp. nov. described here comes from two localities near Villa de Leyva in Boyacá, Colombia, South America (Fig. 1). Most were collected at Loma La Catalina (5° 38' 01" N and 73° 34' 39.94" W), but, one specimen, FCG–CBP 15, was found at the nearby site of Loma La Cabrera (5° 38' 35" N and 73° 36' 22" W). The fossils were preserved in claystone and limestone layers with abundant occurrences of ferruginous-calcareous nodules and concretions, belonging to the middle segment of the Paja Formation called "Arcillolitas abigarradas" (Etayo-Serna 1968), which is upper Barremian-lower Aptian in age (~120 Ma), based on the presence of the *Pseudocrioceras*

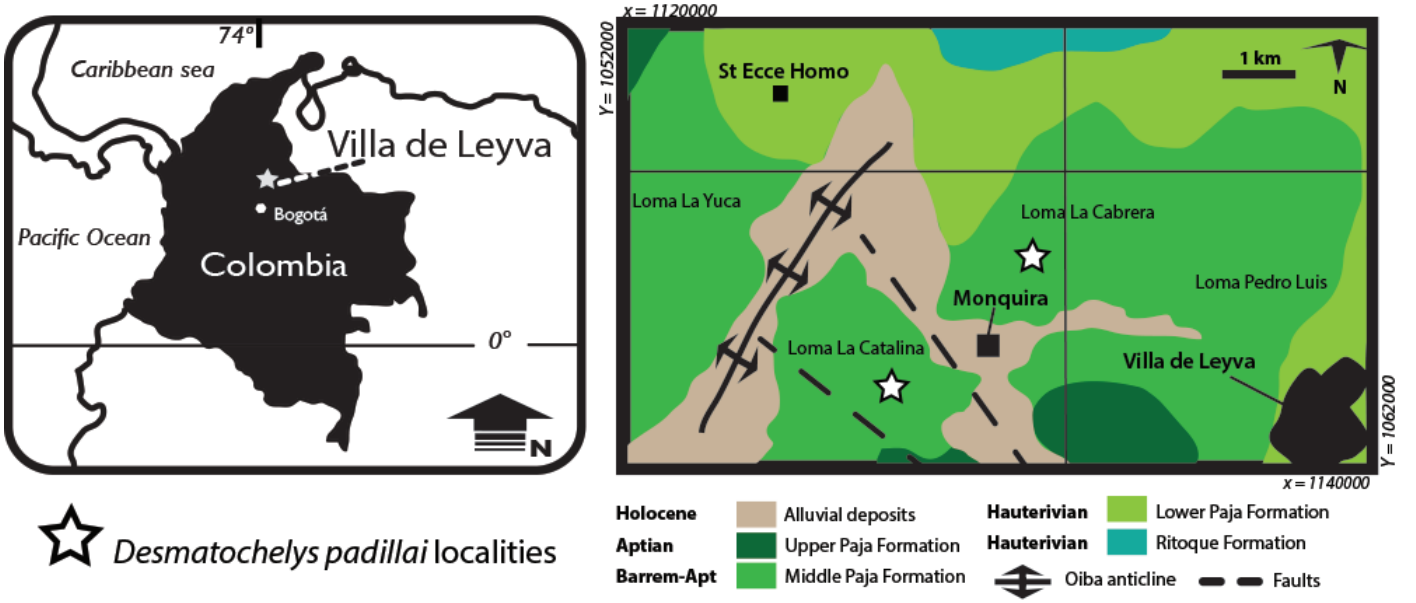

Figure 1. Map showing the location of Villa de Leyva town in Colombia (left) and the geology of the region (right) where *Desmatochelys padillai* was found at the La Catalina hill (Loma La Catalina) and La Cabrera hill (Loma La Cabrera). Geological map redrawn from Hampe (2005).

ammonite assemblage zone (Hoedemaeker 2004). Fossil vertebrates from Villa de Levya include plesiosaurs, pliosaurs, ichthyosaurs, a recently described dinosaur (Carballido et al. in press), fish, and turtles (this study, Cadena in press). All specimens are preserved in a predominantly dark grey limestone. They have a layer of ferruginous oxides that frequently covers the exterior surface of the bones and fills in cavities, which can obscure the sutural contacts between bones. However, this layer can be dissolved with sulfamic acid following the protocol described by Padilla (2011).

All specimens, except those in the University of California Museum of Paleontology (UCMP), were discovered and collected by the local amateur paleontologists Mary Luz Parra and her brothers, Juan and Freddy Parra, who also prepared them at the Centro de Investigaciones Paleontológicas in Villa de Leyva, Colombia (CIP). UCMP specimens were collected from Villa de Leyva, but they lack any additional information about stratigraphic horizon or locality. However, their preservation is identical to all other FCG-CBP material of *D. padillai*, and so far turtles have been only found at the Loma La Catalina site. Taken together, these lines of evidence suggest the UCMP specimens also came from Villa de Leyva.

Phylogenetic analyses

In order to determine the phylogenetic position of *D. padillai* and address the outstanding issues that confound our understanding of fossil marine turtle evolution, we present an updated global character-taxon matrix built from the evaluation, combination, and redefinition of characters and taxa from phylogenetic matrices used for marine turtles (Hirayama 1994, Hirayama 1998, Kear and Lee 2006, Parham and Pyenson 2010, Bardet et al. 2013, Lapparent de Broin et al. 2014b) with global turtle matrices (Joyce 2007, Sterli 2008, Joyce et al. 2011, Anquetin 2012, Rabi et al. 2013, Sterli and de la Fuente 2013, Zhou et al. 2014) (Supplementary Information 1). The final Mesquite matrix can be downloaded at http://escholarship.org/uc/item/147611bv/27300-106320-15-ED.txt. We provide a synonymy for every character in those matrices (Supplementary Information 1). In addition to *D. padillai*, we include 16 of the best-known chelonioids *sensu lato* (the seven extant chelonioids, a fossil stem cheloniid, fossil Pan-*Dermochelys*, *Toxochelys latiremis* Hay, 1908, and six protostegids). We exclude some partially known taxa (i.e., known only from crania or postcrania) and problematic taxa (e.g., *Mongolemys elegans* Khosatzky and Mlynarski, 1971, see Joyce 2007) that are distantly related to chelonioids in all analyses. The final matrix includes 73 taxa and 256 characters (37 ordered) built using Mesquite vers. 3.01 (Maddison and Maddison 2009). Because we focus on marine turtles, three characters from the global matrices (18, 240, 241) are constant and an additional 23 (15, 25, 27, 28, 77, 83, 89, 103-109, 119, 124, 136, 144, 152, 157, 213, 226, 227, 232) are uninformative for our matrix. We report these excluded characters in Supplementary Information 2 for use in future studies and to advance the discussion of global turtle character synonymy.

Two phylogenetic analyses were performed using PAUP* 4.0b10 (Swofford 2002) using a "molecular scaffold" (Springer et al. 2001, Danilov and Parham 2006, Crawford et al. 2015). We based our backbone constraint tree topology for the extant OTUs following the most comprehensive molecular analysis of turtle relationships (Crawford et al. 2015) (Fig. 1S). Analyses were run using the heuristic search algorithm and 1000 random sequence addition replicates.

Our initial analysis included all 233 informative characters and all 73 taxa. We assessed support for each node with a bootstrap analysis of 100 replicates with 10 addition-sequence replicates as well as Bremer indices. In order to investigate the impact of our expanded character list on the position of marine turtles, our second analysis excludes six fossil marine turtles and so includes just the three fossil chelonioid *s.l.* OTUs (*S. gaffneyi*, *T. latiremis*, *Mesodermochelys undulatus* Hirayama and Chitoku, 1996) that were included in Joyce (2007). Table 1S is a list of the extant and fossil taxa examined for this study.

Institutional abbreviations

CIP, Centro de Investigaciones Paleontológicas, Villa de Leyva, Colombia; **FCG–CBP**, Fundación Colombiana de Geobiología, Villa de Leyva, Colombia; **SAMP**, South Australian Museum, Adelaide, Australia; **UCMP**, University of California Museum of Paleontology, Berkeley, California, USA.

SYSTEMATIC PALEONTOLOGY

TESTUDINES Batsch, 1788

PAN-CRYPTODIRA Cope, 1868

CHELONIOIDEA Oppel, 1811 *sensu lato*

PROTOSTEGIDAE Cope, 1872

DESMATOCHELYS Williston, 1894

DESMATOCHELYS PADILLAI sp. nov.

Figs. 2–8

1989 *Desmatochelys lowi* Williston; Smith, p. 158, figs. 7.6-7.8, pls. 7.11-7.15.

1992 *Desmatochelys lowi* Williston; Nicholls, p. 379 (fide Smith).

1997 *Desmatochelys* Williston; Elliot, Irby, and Hutchison, p. 246 (fide Smith).

Diagnosis—*Desmatochelys padillai* is a pan-cryptodire turtle based on the presence of a contact between the

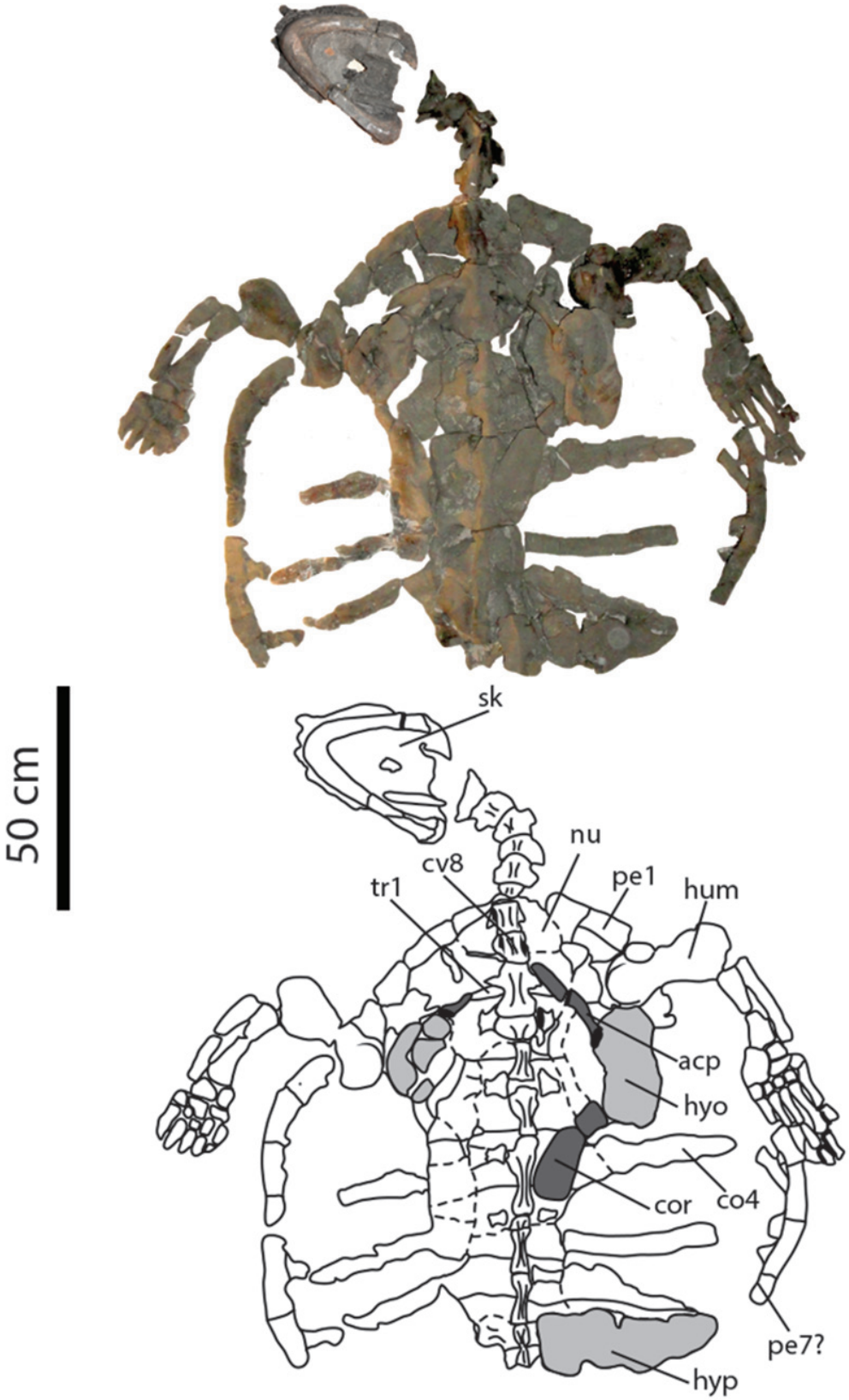

Figure 2. *Desmatochelys padillai* preserved in ventral view, holotype FCG–CBP 01. For the bottom figure; light grey areas represent portions of the plastron and portions of the pectoral girdle are shown in dark grey.

Table 1. Measurements of *Desmatochelys padillai* specimens in millimeters.

Measure	Specimen	Value
Skulls		
Maximum length	FCG–CBP 01	320
	UCMP 38346	308
	FCG–CBP 13	292
	FCG–CBP 15	210
	FCG–CBP 39	181
	FCG–CBP 40	167
Maximum width	FCG–CBP 01	216
	UCMP 38346	213
	FCG–CBP 13	182
	FCG–CBP 15	122
	FCG–CBP 40	110
	FCG–CBP 39	104
Carapace		
Length	FCG–CBP 01	1660
Length estimated for complete carapace		2000
Width		1353
Width estimated for complete carapace		1355
Thickness average of carapace measured in neurals, costals and peripherals		15

pterygoid and the basioccipital (Character 64). It is a protostegid based on the: 1) jugal-quadrate contact (Character 21); 2) pterygoids, extending laterally almost reaching the mandibular condyle facet (Character 75); 3) humerus, with a lateral process expanding onto ventral surface (Character 240); 4) radius curves anteriorly (Character 247). Within Protostegidae, *D. padillai* can be diagnosed from all protostegids by: 1) a larger nasal opening facing anteriorly in dorsal view compared to other protostegids; 2) wider pterygoids in ventral view; 3) wider ventral process of cervicals, with a flat to slightly concave ventral surface; 4) dorsal surface of neurals smooth without keels and having a medial shallow depression; and 5) centrale bone rectangular and elongated in shape. *Desmatochelys padillai* resembles *Bouliachelys suteri* Kear and Lee, 2006 by having a globular posteriormedial roof of the skull, which is flatter in all other protostegids. *Desmatochelys padillai* shares with *Desmatochelys lowi* Williston, 1894 a long transversal process of cervicals that is rectangular in shape, positioned at the central region of the vertebra. This character is in contrast to the shorter more anteriorly positioned transverse process of other chelonioids *s.l. Desmatochelys padillai* shares with *D. lowi* and cheloniids the absence of foramen jugulare posterius.

Holotype—FCG–CBP 01 (Figs. 2–5, Table 1). A complete skull, lower jaw, partial right hyoid, cervical vertebrae (3–8), right and left forelimbs (missing most phalanges), nearly complete carapace, left scapula and coracoid, partial hyoplastron and hypoplastron.

Referred Specimens—UCMP 38346 (Fig. 6), complete, articulated skull and lower jaw, adult individual. FCG–CBP 40 (Fig. 7), complete articulated skull and lower jaw, juvenile specimen. FCG–CBP 13 (Fig. 8A–F), nearly complete articulated skull and lower jaw, adult specimen. FCG–CBP 39 (Fig. 8G–J), nearly complete articulated skull and lower jaw, juvenile specimen. UCMP 38345A (Fig. 9A, B) midline portion of the carapace, neurals 2–8 complete and most of the medial portion of costals. UCMP 38345B (Fig. 9C–E), posterior portion of the carapace with complete 8–9? neurals and suprapygal, and the medial portion of the three most posterior costal pairs. FCG–CBP 15, nearly complete articulated skull and lower jaw, badly preserved, juvenile specimen.

Etymology—Specific epithet is in honor of the late Carlos Bernardo Padilla, who led and supported the paleontological projects at Villa de Leyva, and also helped find the FCG-CBP specimens.

Occurrence and Age— Loma La Catalina and Loma La Cabrera, near Villa de Leyva in Boyacá, Colombia, South America, Paja Formation, Late Cretaceous (upper Barremian-lower Aptian, ~120 Ma).

DESCRIPTION AND COMPARISONS

We describe and compare *Desmatochelys padillai* to other chelonioids *s. l.*, especially protostegids such as *Archelon ischyros* Wieland, 1896, *B. suteri*, *D. lowi*, *Protostega gigas* Cope, 1872, *Rhinochelys* Seeley, 1869, and the aforementioned *S. gaffneyi*, but also to the stem chelonioid *Toxochelys latiremis* and other chelonioids *s.l.* We combine the description and comparisons into a single section, thereby avoiding repetition of text. The description presented here corresponds to the general morphology for *D. padillai* based on all the referred skulls. Small differences in bones proportions, shapes or length of sutural contacts between the skulls are considered as part of intraspecific variations or effects of crushing or preservation and are not detailed here.

Figure 3. *Desmatochelys padillai* skull, holotype FCG–CBP 01. A, B, dorsal view. **C, D,** ventral view. **E, F,** left lateral view. Abbreviations: **an**: angular, **ar**: articular, **de**: dentary, **fr**: frontal, **hy**: hyoid; **mx**: maxilla, **na**: nasal, **pa**: parietal, **pf**: prefrontal, **pm**: premaxilla, **po**: postorbital, **qj**: quadratojugal, **qu**: quadrate, **sq**: squamosal, **su**: surangular. ▶

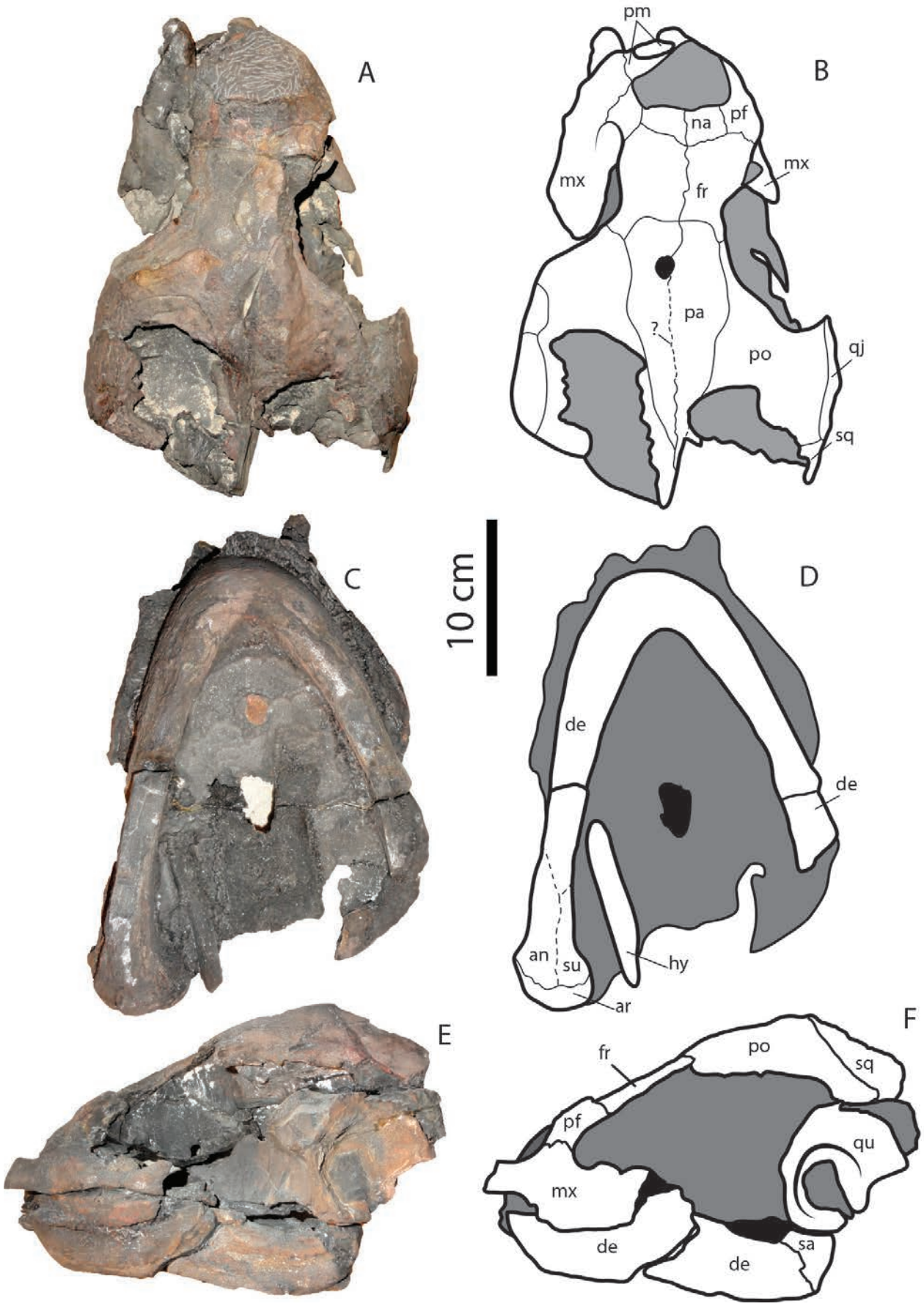
A
B
pm
na
pf
mx
mx
fr
pa
?
po
qj
sq
C
10 cm
D
de
de
an
su
hy
ar
E
F
fr
po
sq
pf
qu
mx
de
de
sa

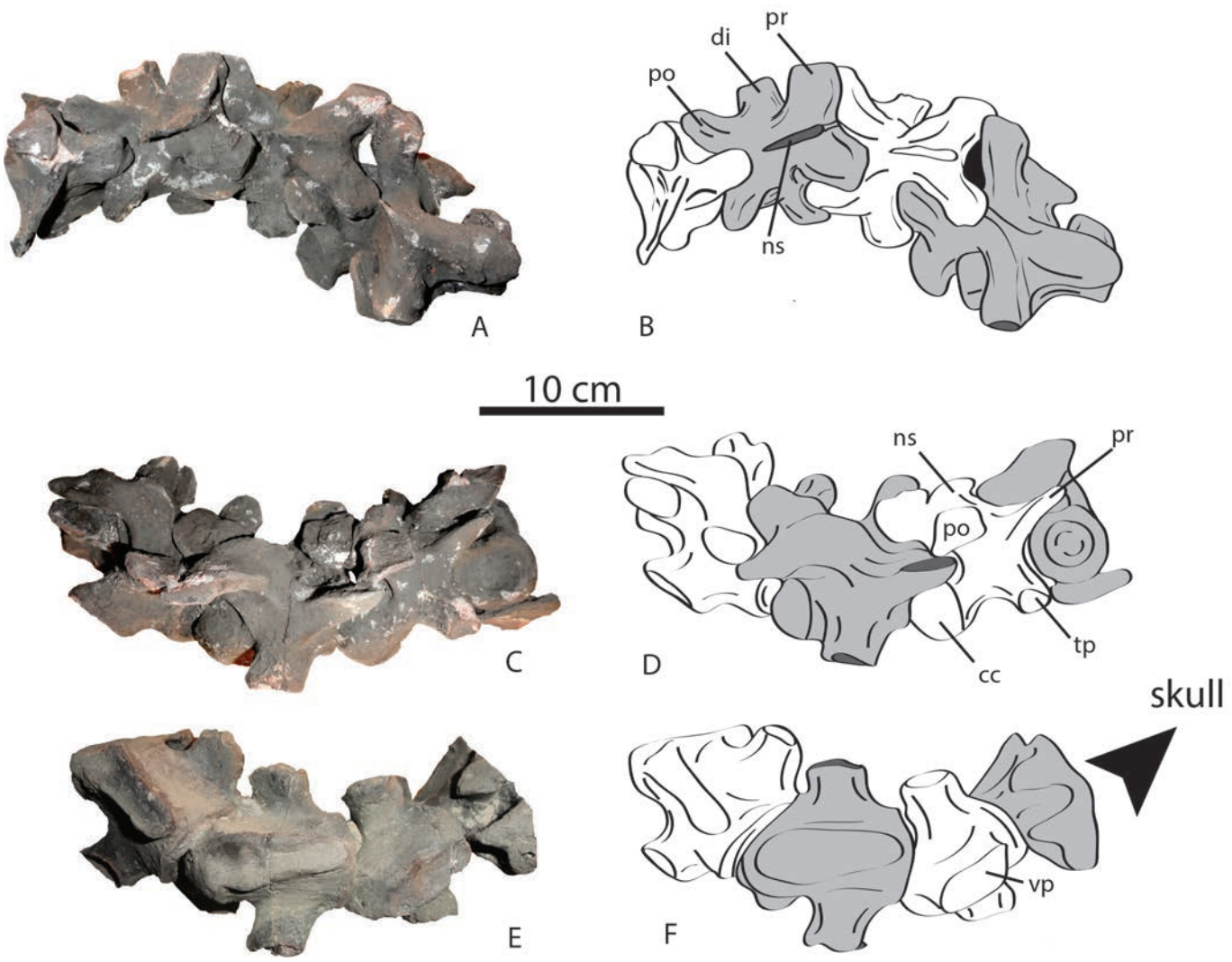

Figure 4. *Desmatochelys padillai.* Cervical vertebrae 4 to 7, holotype FCG–CBP 01. **A, B**, dorsal view. **C, D**, left lateral view. **E, F**, ventral view. Abbreviations: **cc**: cervical condyle, **di**: diapophysis, **ns**: neural spine, **po**: postzygapophysis, **pr**: prezygapophysis, **tp**: transverse process, **vp**: ventral process.

Description

Skull dorsal view—In dorsal view (Figs. 3A, B; 6E, F; 7A, B; 8C, D, I, J), nasal bones are present (Character 1), triangular to square in shape, and contact each other medially (Character 2) with a reduced exposure in contrast to the size of the frontals (Character 3), and exclude medial contact between prefrontals (Character 4). The nasal opening is relatively large and faces more anteriorly than dorsally compared to all other protostegids. The prefrontals are reduced in their dorsal exposure (Character 7) and like the frontals and parietals lack defined cranial scale sulci (Character 8). The frontals reach the orbits laterally (Character 10), contact the prefrontals anteriorly and the parietals and postorbitals posteriorly. The orbits are large and face dorsolaterally (Character 12). The parietals contact the postorbitals laterally and frontals anteriorly, do not contact the squamosals. Although none of the skulls preserves the original edge of the temporal emargination, it seems that it was moderately developed (Character 13). The frontals, parietals, and postorbitals of *D. padillai* have radial striations on the dorsal surface of the bone similar, though slightly less defined, to those seen in the Late Cretaceous protostegid *D. lowi*. Also like *D. lowi*, specimens of *D. padillai* have a well-defined pineal foramen (Character 18) located at the sutural contact between parietals and frontals. At the roof of the otic chamber, the prootic contacts the ophistotic, and the foramen stapedio-temporalis (Character 17) is located at the triple suture between the quadrate, the prootic, and the opisthotic, as in *D. lowi* and

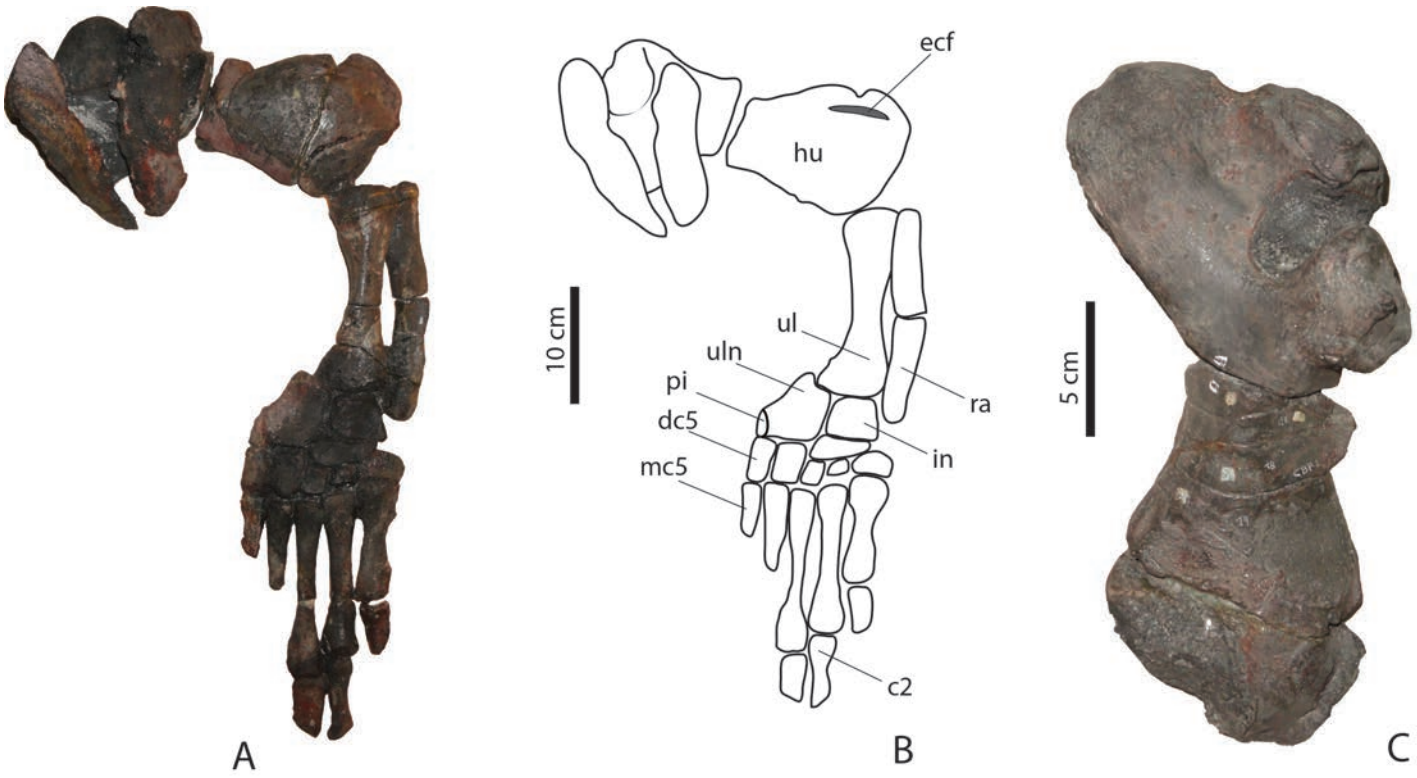

Figure 5. *Desmatochelys padillai*. Left paddle, holotype FCG–CBP 01. **A, B**, dorsal view. **C**, left humerus isolated in ventral view. Abbreviations: **c2**: carpal 2, **ecf**: foramen ectepicondylaris, **dc5**: distal carpal 5, **hu**: humerus, **in**: intermedium, **mc5**: metacarpal 5, **pi**: pisiform, **ra**: radius, **ul**: ulna, **uln**: ulnare.

B. suteri. The roof of the otic chamber is usually hidden by the roof of the skull in dorsal view, and so is poorly known for all other protostegids. The crista supraoccipitalis is very long and narrow, and protrudes posterior to the foramen magnum (Character 76), a characters that is variable among chelonioids *s.l.*

Skull ventral view—In ventral view (Figs. 6G, H; 7C, D; 8G, H), *D. padillai* exhibits a large vomer that contacts the palatines posteriorly (Characters 44 and 45). As in all other protostegids, *D. padillai* lacks a secondary palate (Character 40), which is present in all other chelonioids *s.l.* except *T. latiremis* and *Eochelone brabantica* Dollo, 1903. *Desmatochelys padillai* has a large foramen palatinum posterius (Character 66) that opens posterolaterally, as in *S. gaffneyi*, *B. suteri*, and *Rhinochelys pulchriceps* Owen, 1842. A smaller foramen palatinum posterius is characteristic of *D. lowi*. and it is completely absent in all other chelonioids *s.l.* except for *T. latiremis* and *Nichollsemys bairei* Brinkman, Hart, Jamniczky, and Colbert, 2006. A clearly defined foramen orbitonasale is present at the most anterior region of the palatine in *D. padillai* specimen FCG–CBP 39. In contrast to other protostegids, the pterygoids of *D. padillai* are widest at the level where they contact the basisphenoid. The processus pterygoideus externus is reduced forming an acute tip (Character 72), similar as in all other protostegids and *T. latiremis*. The pterygoids lack the posterolateral pockets present in extant cheloniids, however they exhibit circular, variably-sized pterygoid pits close to the suture with the basisphenoid, as in extant cheloniids. Posterolaterally, pterygoids reach the level of the condylar facet (Character 75), as in all other protostegids. The basisphenoid is triangular in shape, lacks the lateral keels present in *B. suteri* and *D. Lowi*, and has a flat ventral surface, in contrast to the V-shaped crest of pan-cheloniids (Character 88). The foramen posterior canalis carotici interni (Characters 99 and 100) (see Rabi et al. 2013 for foramina definitions) is visible lying between the basiphenoid, basioccipital, and pterygoid contact, as in chelonioids. For protostegids, the condition is still poorly documented or remains unclear, and requires the direct examination of fossil specimens that was not feasible for this study. The basioccipital of *D. padillai* is wider than long, contacts the basisphenoid anteriorly, pterygoids laterally, and exoccipitals dorsally, lacks anterior tubercles (Character 80), and has very short and rounded posterolateral processes.

Skull lateral view—In lateral view (Figs. 3E, F; 6A, B; 7G, H; 8A, B, E), *D. padillai* exhibits a large, almost circular

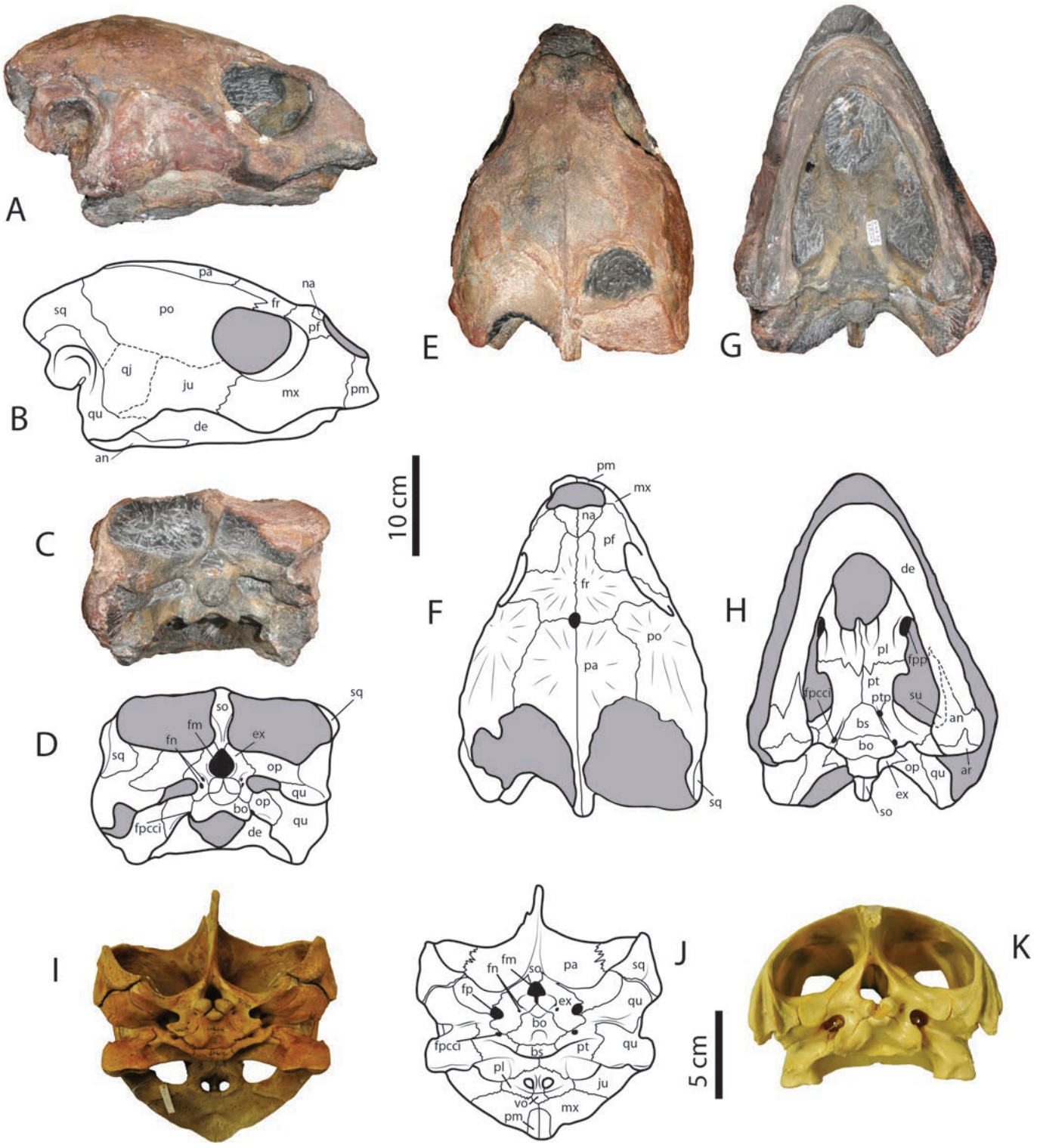

Figure 6. A-H. *Desmatochelys padillai.* Skull, UCMP 38346. **A, B**, right lateral view. **C, D**, posterior view. **E, F**. Dorsal view. **G, H**, ventral view. **I, J**. Extant cheloniid *Caretta caretta.* Posterior view of skull, USNM 317907. **K**. Extant cheloniid *Chelonia mydas.* Posterior view of skull, FMNH 211910. Abbreviations: **an**: angular, **ar**: articular, **bs**: basisphenoid, **bo**: basioccipital, **de**: dentary, **ex**: exoccipital, **fm**: foramen magnum, **fn**: foramen nervi hypoglossi, **fp**: fenestra postotica, **fpcci**: foramen posterius canalis carotici cerebralis, **fr**: frontal, **hy**: hyoid; **ju**: jugal, **mx**: maxilla, **na**: nasal, **op**: opisthotic, **pa**: parietal, **pf**: prefrontal, **pl**: palatine, **pm**: premaxilla, **po**: postorbital, **pt**: pterygoid, **ptp:** pterygoid pits, **qj**: quadratojugal, **qu**: quadrate, **sq**: squamosal, **so**: supraoccipital, **su**: surangular, **vo**: vomer.

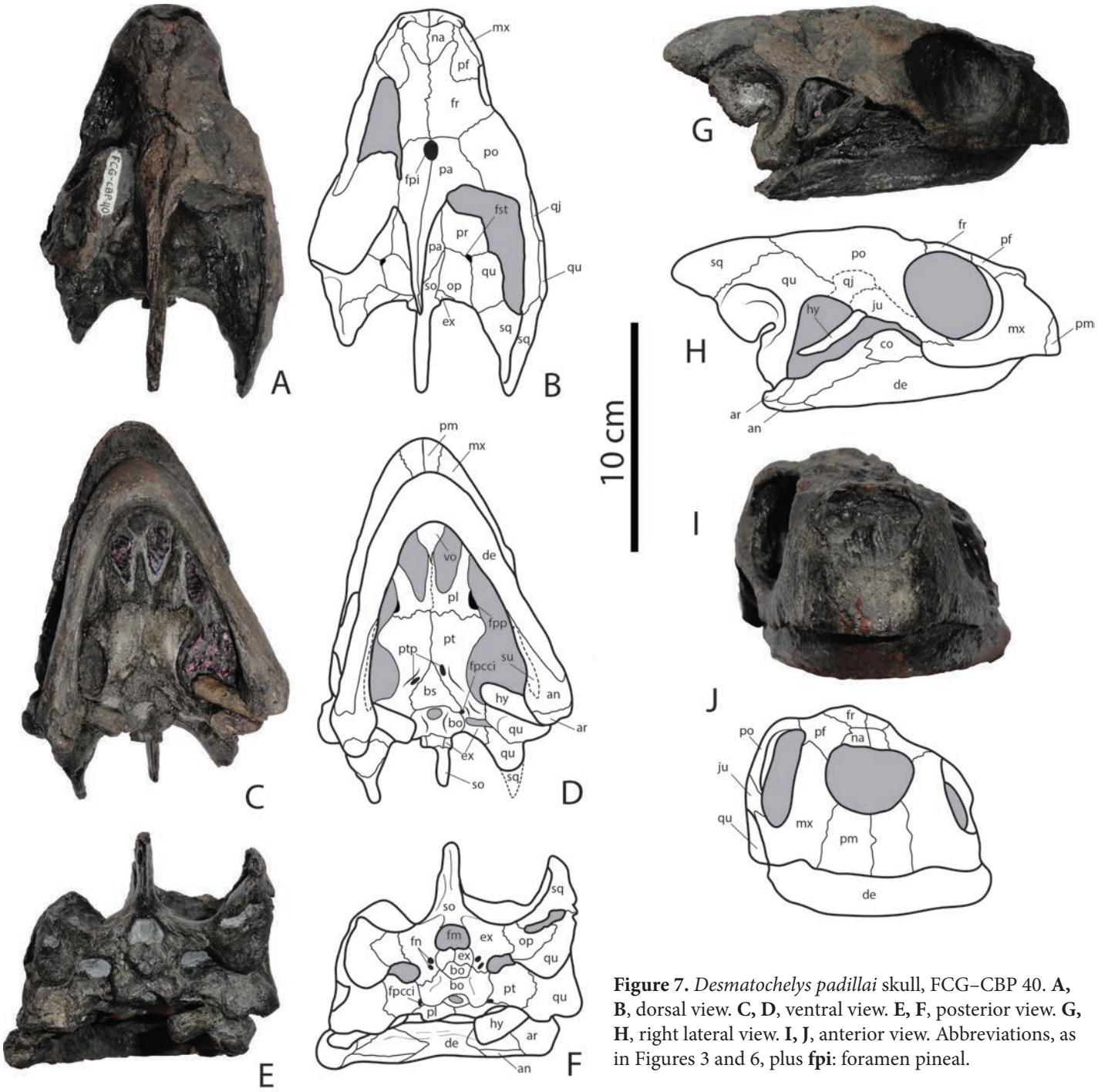

Figure 7. *Desmatochelys padillai* skull, FCG–CBP 40. **A, B**, dorsal view. **C, D**, ventral view. **E, F**, posterior view. **G, H**, right lateral view. **I, J**, anterior view. Abbreviations, as in Figures 3 and 6, plus **fpi**: foramen pineal.

orbital opening (Character 12), ontogenetically conservative (same proportional size and shape in juveniles and adults), creating a very narrow lateral exposure of the interorbital bar (formed by the prefrontal and frontal) similar to *S. gaffneyi,* and *Rhinochelys* spp. In these taxa, the condition could be due to the very early ontogenetic stage of the available specimens, which is also the case of extant cheloniid species. In *D. padillai*, the large orbits are retained even in the adults. *Desmatochelys lowi* and other chelonioids *s.l.* have smaller orbits in adult stages. Lower cheek emargination (Character 23) is very shallow to almost absent resembling all other protostegids (see fig. 2 in Hirayama 1994). A contact between the quadrate and the jugal (Character 21) is present in *D. padillai* as in all other protostegids for which these two bones are preserved. *Desmatochelys padillai* lacks squamosal-jugal contact (Character 19). The posterior roof of the skull

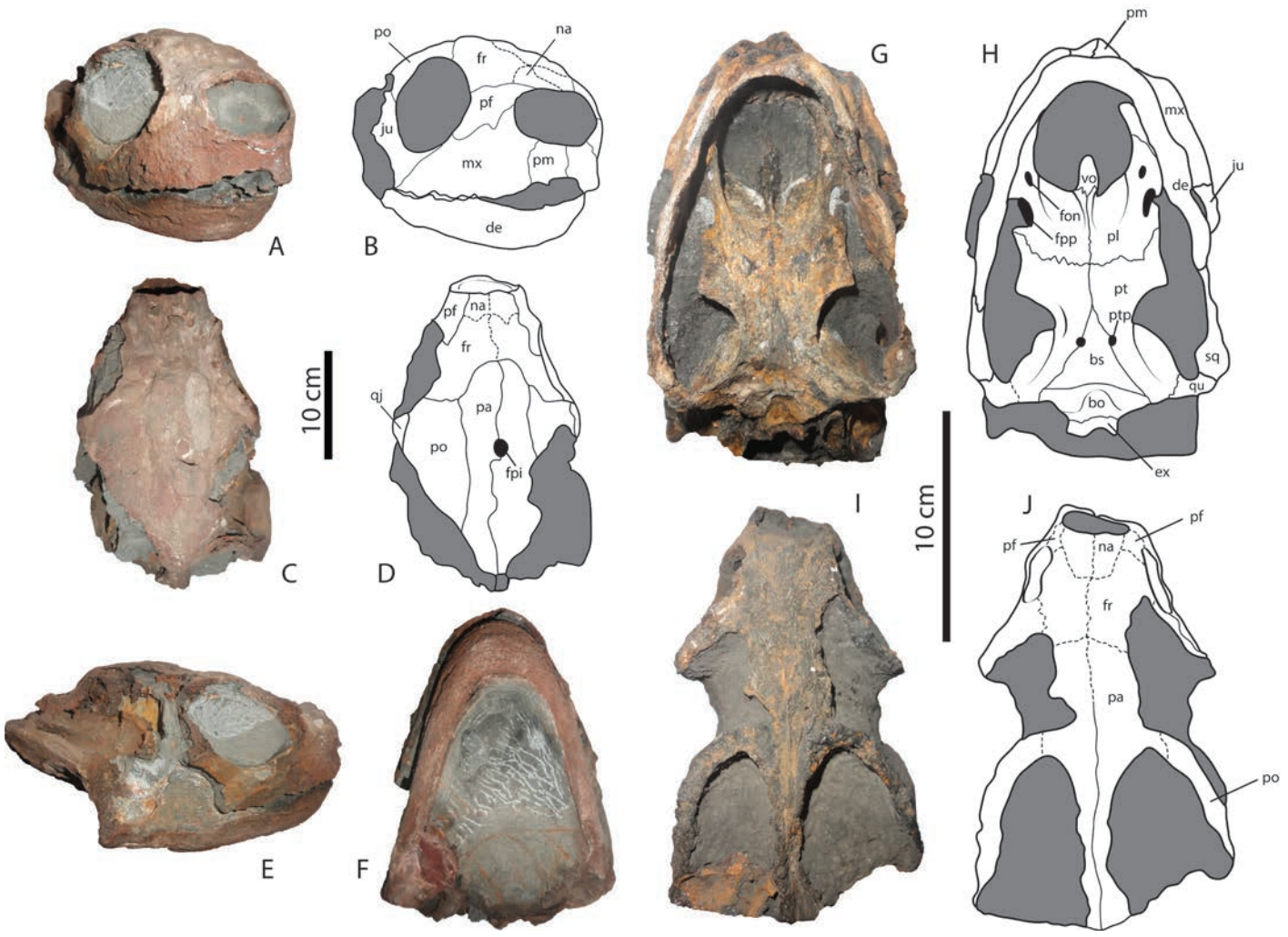

Figure 8. *Desmatochelys padillai.* Skull, CG–CBP 13. **A, B**, anterolateral view. **C, D**, dorsal view. **E**, right lateral view. **F**, ventral view. *Desmatochelys padillai* skull, FCG–CBP 39. **G, H**, ventral view. **I, J**, dorsal view. Abbreviations as in Figure 6 plus **fon:** foramen orbito-nasale

is slightly globular, similar to *B. suteri,* in contrast to *D. lowi* and *Rhinochelys* spp., which have a flatter posterior roof of the skull. The cavum tympani (Character 53) is circular in outline with the incisura columellae auris open as in all other chelonioids. The antrum postoticum is small in *D. padillai*, and fully enclosed anteriorly by the quadrate (Character 55).

Skull posterior view—The posterior view of the skull of *D. padillai* (Figs. 6C, D; 7E, F), resembles in all aspects and bone contacts the skull of extant cheloniids (Fig. 6I–K). The exoccipitals contact the opisthotics laterally, the supraoccipital dorsally, and the basioccipital ventrally. The occipital condyle is formed by the contribution of the basioccipital and both exoccipitals. At the exoccipital, *D. padillai* lacks the foramen jugulare posterius as in *D. lowi* and chelonioids, this is due to its confluence within the fenestra postotica. The foramen magnum in *D. padillai* is slightly wider than long, both foramina nervi hypoglossi are clearly visible in both sides of exoccipitals, located very close to the occipital condyle. The fenestra postotica is slightly larger than that in extant cheloniids and is encapsulated between opisthotic, exoccipital, and quadrate. Unfortunately, the posterior view of the skull is poorly documented for protostegids, limiting the comparison between taxa and the identification of diagnostic characters.

Lower jaw—As in *D. lowi, Rhinochelys nammourensis* Tong, Hirayama, Makhoul, and Escuillié, 2006*, S. gaffneyi,* and *Terlinguachelys fischbecki* Lehman and Tomlinson, 2004 the angle of separation between both rami in *D. padillai* is ~60º; a wider angle is present in cheloniids (>60º) whereas a much narrower angle (~40º) is present in the other protostegids (see fig. 3 in Lehman and Tomlinson 2004). In lateral view (Fig. 7G, H) the processus coronoideus has a very low dorsal projection as in other protostegids and *T. latiremis* (see fig. 3 in Lehman and Tomlinson 2004). This short

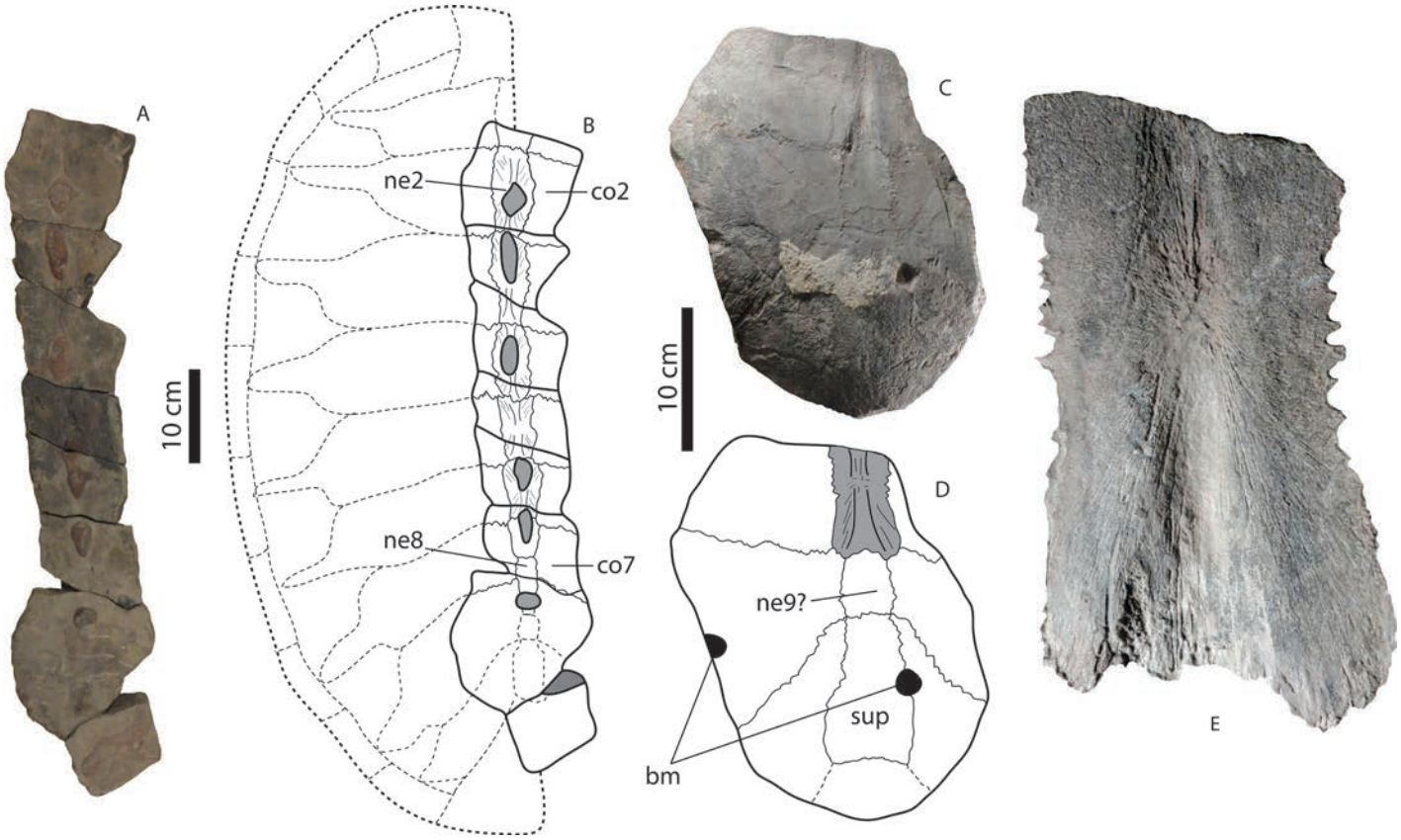

Figure 9. *Desmatochelys padillai* carapace fragments. **A**, UCMP 38245A in dorsal view including neurals 2-8, and the medial portion of costals. **B**, a hypothetical carapace reconstruction based on UCMP 38245A. **C, D**, UCMP 38245B specimen in dorsal view, posterior portion of the carapace, including neurals 8-9? and suprapygal. **E**, close up of neural bone, colored grey in D. Abbreviations: **bm**: bite marks, **co**: costal, **ne**: neural, **sup**: suprapygal. Grey oval shadows in B represent ferruginous nodules.

projection indicates a more reduced area for the insertion of the adductor mandibulae externus Pars superficiales lateral muscle and a probably much longer adductor mandibule externus Pars profundus muscle than in extant cheloniids (see fig. 9 in Jones et al. 2013 for muscles terminology and illustration). Cheloniids have a procesuss coronoideus that is more dorsally projected forming an obvious convexity in lateral view. The contacts between the surangular, angular, and dentary are not clearly defined in *D. padillai*, as well as the presence or absence of the splenial bone.

Cervical vertebrae—Desmatochelys padillai has cervicals (4 to 8 series) with narrow and low dorsal processes of the neural arch. All cervicals are preserved in articulation (Fig. 4A, B). Both the pre- and postzaygapophyses are low. The prezygapophyses project dorsolaterallly and the postzaygapophyses project ventrolaterally. The transverse process (Character 186) is located along the midline of the centrum as in *D. lowi* (see pl. 1H in Zangerl and Sloan 1960), ending in a flat to concave facet, and being almost square-rectangular in shape in ventral view (Fig. 4E, F).

The cervicals of *D. padillai* have a thick ventral process (keel) that is oval in shape and ventrally flat to slightly concave (Fig. 4E, F), being slightly more robust in cervicals 6 and 7. The ventral process in *D. lowi* and other chelonioids *s.l.* is much narrower and with a convex surface. The wide and flat to slightly concave morphology of the ventral process suggests a very strong and large surface for attachment of the tendons of the longus colli Partes capitis muscle that runs ventrally along the neck of extant cheloniids (see fig. 12 in Jones et al. 2013). The central articulation of cervicals 4 to 8 (Character 188–198) are all of the ball and socket type, procoelous, and almost circular in outline. Cervical 4 is slightly longer than cervicals 5 to 8, cervical 8 is the shortest, having an elongated and curved left postzygapophysis. This particular feature of cervical 8 has been considered the most common condition in crown cryptodires (Joyce 2007). In all these aspects, the cervicals of *D. padillai* resemble the cervicals of *D. lowi* and cervical 5 of *Protostega dixie* Zangerl, 1953a (Fig. 53). In cheloniids and *D. coriacea,* the articulations between cervicals 6 to 8 are wider than high and cervicals 7 and 8 (Character 198) have double articulations.

Front paddle—The humerus of *D. padillai* is robust with the processus medialis almost at the same level of the caput humeri (Characters 237–240). The processus lateralis is located anteriorly very close to the caput humeri, and the foramen ectepicondylaris is deep and particularly visible on the left front paddle. In all these characters, the humerus of *D. padillai* resembles the humeri of other protostegids (See fig. 6 in Hirayama 1994 and Fig. 8 in Lehman and Tomlinson 2004). The radius is longer than the ulna, slightly convex anteriorly as in all other protostegids (Character 247). The ulnare is pentagonal in shape and larger than the intermedium, which is squared (Character 251). The centrale is rectangular in shape and contacts distal carpals 1 to 4 posterolaterally; the centrale of all other chelonioids *s.l.* is circular to slightly oval in shape. Distal carpals 5 and 4 are square in shape and larger than the other three distal carpals, all five distal carpals are almost the same size as those in all other protostegids and chelonioids. Metacarpal 3 is slightly longer than 2 as in all other protostegids whereas it is variable in other chelonioids *s.l.* (see fig. 9 in Tong et al. 2006).

Shell and pectoral girdle—Desmatochelys padillai has an oval carapace with a convex anterior margin. Unfortunately, the dorsal surface of the carapace of the holotype is badly preserved, without any recognizable sutures or sulci. There are nine rectangular neurals with medial depressions and surface striations in UCMP 38345A, the specimen found associated with UCMP 38346 (a skull), as well as neurals found with the holotype. In *D. lowi,* and all other protostegids for which neurals are known, dorsal keels are present, which can also be developed in cheloniids (e.g., *Caretta caretta* [Linnaeus,1758]). The peripherals of *D. padillai* are much longer than wide as in all other protostegids and some cheloniids (e.g., *Chelonia mydas* [Linnaeus, 1758]). *Desmatochelys padillai* has a long, slightly trapezoidal, suprapygal bone, with the sulcus between vertebral scales 4 and 5 located over its anterior portion, observed in UCMP 38345B (Fig. 9C, D). Two circular and deep bite marks are present in UCMP 38345B (Fig. 9C, D) potentially caused by pliosauroids, which are very abundant in the sequence of Paja Formation in Villa de Leyva (Hampe 2005). The first thoracic rib is short (Fig. 10), differing from the conclusion of Joyce (2007) that protostegids have a very elongated first thoracic rib as in primitive Testudines, and restricting that condition to *S. gaffneyi*. Only two portions of the plastron are preserved, a fragment each of the left hyoplastron and hypoplaston. These elements are too poorly preserved to reconstruct their original plastron shape. The acromial process of the scapula has a blade shape, wider distally, with a slightly convex dorsal surface (Fig. 10). The acromial process is cylindrical with dorsal striations on the most distal portion. In all these aspects the pectoral girdle elements of *D. padillai* resemble those from other protostegids (see fig. 8 in Lehman and Tomlinson 2004), with the main difference being that the scapular process is shorter and thicker in *A. ischyros* and *P. gigas.*

PHYLOGENETIC RESULTS

Our primary analysis results in a single tree of 900 steps (Fig. 11). For the purpose of this study we focus our discussion to the placement of chelonioids and their hypothesized closest relatives. As constrained with our molecular scaffold, chelonioids are placed as the sister taxon to Chelydroidea Baur, 1893 (*sensu* Knauss et al. 2011) within the Americhelydia Joyce, Parham, Warnock, and Donoghue, 2013. Within this framework of extant lineages, fossil taxa assigned to three extinct groups of cryptodires with plesiomorphic characters (Macrobaenidae Sukhanov, 1964 [Cretaceous to Paleocene], Sinemydidae Yeh, 1963 [Early Cretaceous], Xinjiangchelyidae Nessov in Kaznyshkin, Nalbandyan, and Nessov, 1990 [Jurassic]; see phylogenetic definitions for all three groups in Rabi et al. 2014) are united into a monophyletic group on the stem of Chelonioidea (Pan-Chelonioidea, Fig. 11). Our analysis also places two Jurassic forms (*Solnhofia parsonsi* Gaffney, 1975 and *Jurassichelon oleronensis* Pérez-García, 2015 inside Pan-Chelonioidea), though more crownward than the macrobaenid - sinemydid - xinjiangchelyid grouping. The stem chelonioid *T. latiremis* is considered the sister taxon to a clade formed by Cheloniidae + Protostegidae + Pan-*Dermochelys*. Within the Chelonioidea *s.l.*, protostegids are placed as the sister taxon to Pan-*Dermochelys*. Within the protostegids, *S. gaffneyi i*s the most basal taxon, whereas *D. padillai* is placed as the sister taxon to *D. lowi* consistent with its earlier referral to that species (Nicholls 1992, Elliot et al. 1997). The *D. lowi* and *D. padillai* clade is placed as the sister taxon to a Late Cretaceous clade that includes *R. nammourensis, A. ischyros,* and *P. gigas.*

Our analysis placed the protostegids on the stem of *D. coriacea*, i.e., within Chelonioidea. This topology is similar to that found by previous analyses of chelonioid phylogeny (Hirayama 1994, Hirayama 1998, Kear and Lee 2006, Bardet et al. 2013), but differs from the global analysis of Joyce (2007), which placed *S. gaffneyi*, and ostensibly all other protostegids, outside of Chelonioidea. Because our data matrix included both more characters and more taxa than Joyce (2007), we ran an analysis including the same three fossil chelonioids *s.l.* as that study. Unlike Joyce (2007), our results also included protostegids (represented by *S. gaffneyi*) close to Chelonioidea, although this time on the stem and not within the crown. Based on this result, we conclude that the placement of *S. gaffneyi* (and by extension all other protostegids) results from the inclusion of the characters from more

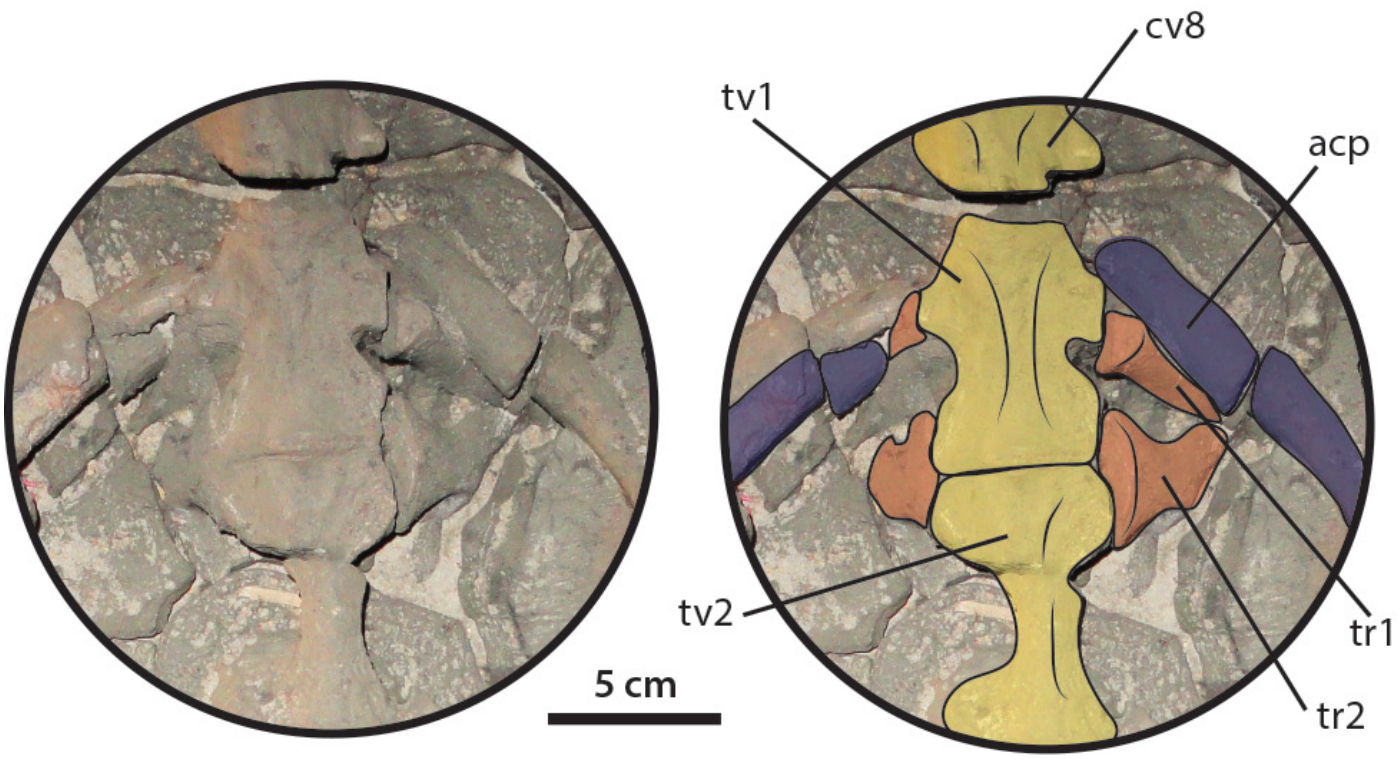

Figure 10. *Desmatochelys padillai*. The most anterior portion of the carapace close-up in ventral view showing the arrangement of the first two thoracic vertebrae and thoracic ribs, holotype FCG–CBP 01. Abbreviations: **acp**: acromion process, **cv**: cervical vertebra, **tr**: thoracic rib, **tv**: thoracic vertebra.

restricted (marine turtle) phylogenetic data matrices (i.e., Hirayama 1994, Hirayama 1998, Kear and Lee 2006, Parham and Pyenson 2010, Bardet et al. 2013, Lapparent de Broin et al. 2014b). The implications of this result are discussed below.

DISCUSSION

A phylogenetic definition for Protostegidae

The monophyly and content of Protostegidae has been demonstrated by previous authors (Zangerl 1953a, Hirayama 1994, 1998, Hooks 1998, Kear and Lee 2006) and is supported by our analysis. Therefore, we define Protostegidae as the most inclusive clade that includes *Protostega gigas*, but no living turtle or the 'essential' members of Macrobaenidae, Sinemydidae or Xinjiangchelyidae (i.e., *Macrobaena mongolica* Tatarinov, 1959, *Sinemys lens* Wiman, 1963, and *Xinjiangchelys junggarensis* Yeh, 1986). This definition is modeled from a recent study that phylogenetically defined three clades of fossil pan-cryptodires (Rabi et al. 2014). Because the ultimate phylogenetic position of protostegids within Pan-Cryptodira is unknown (see below), it is necessary to ensure that our definition does not overlap with these previously defined fossil clades.

Polyphyly of marine turtles?

The placement of *D. padillai* and other protostegids within Chelonioidea in our study is driven by the inclusion of characters from marine turtle matrices into global matrices (see Phylogenetic Results). This matches the traditional position of protostegids, and in contrast to recent studies assert that protostegids are not chelonioids, but rather an independent marine radiation (Joyce 2007, Joyce et al. 2013, Parham et al. 2014). An in-depth study of how marine turtle characters/homoplasies are affecting the topology is beyond the scope of this paper. However, because the resolution of these competing hypotheses determines whether *D. padillai* is the oldest known chelonioid, and hence a good fossil calibration for molecular studies, we review some of the attendant issues and relevant patterns below.

The results of our cladistic analysis place two grades of extinct turtles near the base of the chelonioid stem Jurassic marine turtles and a grouping of primarily Jurassic and Cretaceous freshwater cryptodires with plesiomorphic characters (i.e, macrobaenids, sinemydids, and xinjiangchelyids). The latter result was also obtained by Sterli (2010). The freshwater forms are placed as the sister taxon to all other pan-chelonioids. Because these taxa are largely characterized by a lack of

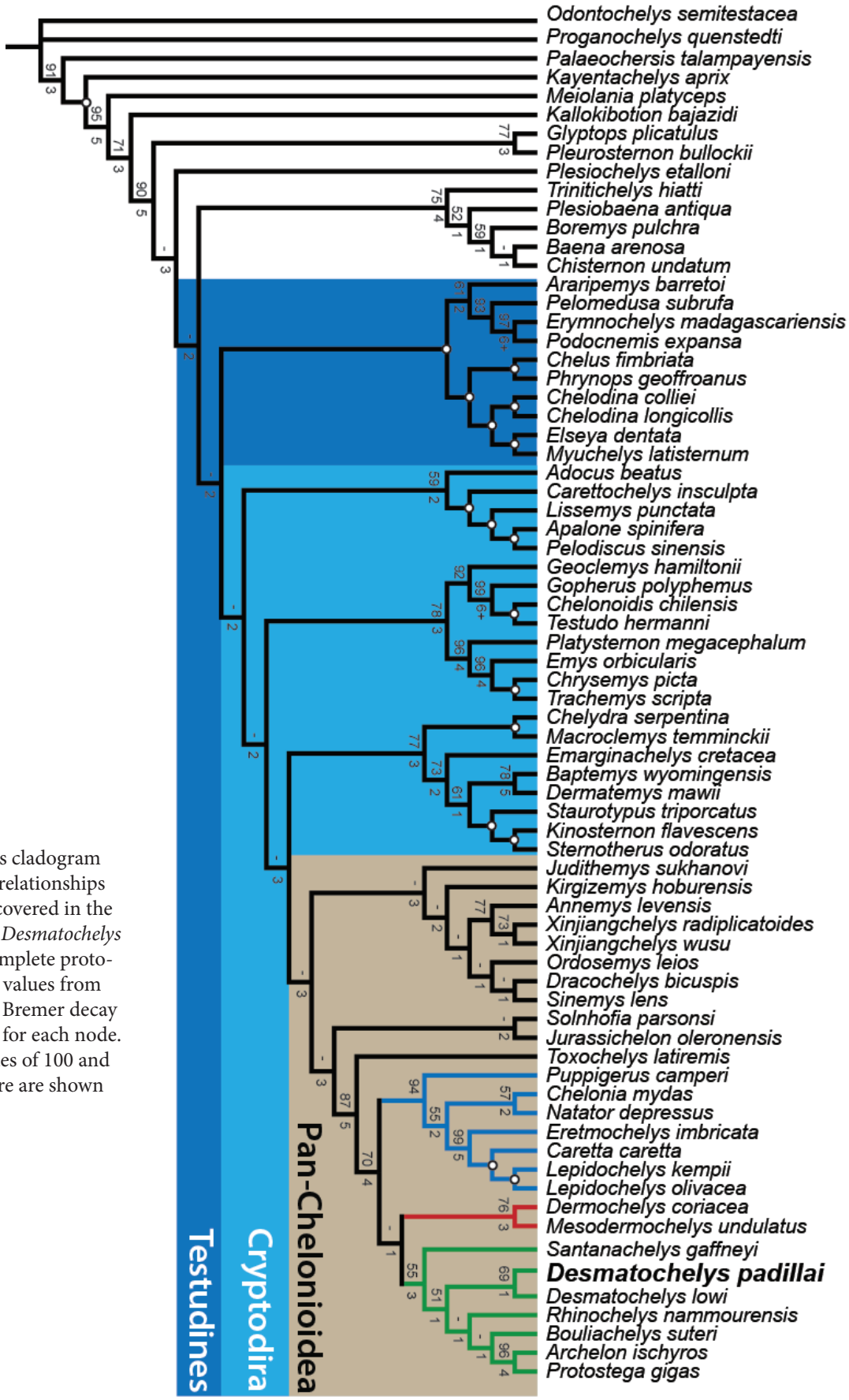

Figure 11. Strict consensus cladogram showing the phylogenetic relationships between marine turtles recovered in the current analysis including *Desmatochelys padillai* and other most complete protostegids. Bootstrap support values from 100 replicates (above) and Bremer decay indices (below) are shown for each node. Nodes with bootstrap values of 100 and Bremer indices of 6 or more are shown with an open circle.

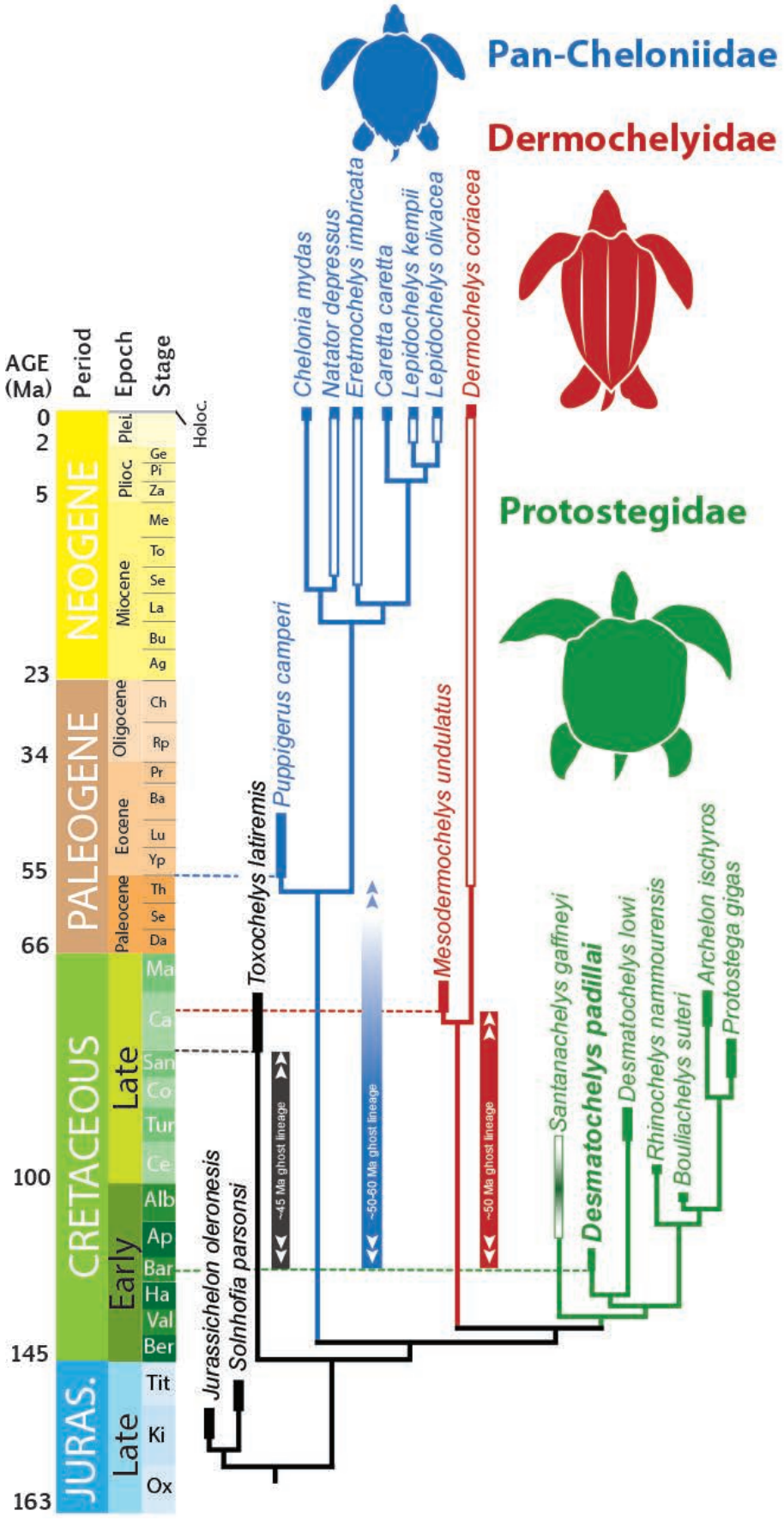

Figure 12. Chronostratigraphic distribution of Pan-Chelonidoidea clade matching the topology presented in Figure 11. Solid square-rectangles at the tip branches are based on the fossil occurrences. White rectangles represent fossils that show the age of the stem lineages. The data for these are from Parham and Pyenson (2010) with a correction to the age of crown group cheloniids to Zanclian instead of Serravalian. Note that some taxon ranges are long due to stratigraphic uncertainty and should not be interpreted as illustrating a continuous fossil record. For *S. gaffneyi* we use a gradient fill to emphasize this. Taxon ranges for fossil occurrences were taken from literature as follows, starting from the left: *Jurassichelon oleronesis* from Pérez-García (2015), *Solnhofia parsonsi* from Joyce (2000), *Toxochelys latiremis* from Hirayama (1997), see also Joyce et al. (2013), *Puppigerus camperi* from Moody (1974), *Mesodermochelys undulatus* from Hirayama and Chitoku (1996) and Hirayama et al. (2006), *Santanachelys gaffneyi* from Hirayama (1998) see also Martill (2007) and Joyce et al. (2013), *Desmatochelys padillai* from this study, *Desmatochelys lowi* from Elliot et al. (1997) and Hirayama (1997), *Rhinochelys nammourensis* from Tong et al. (2006), *Archelon ischyros* from Hirayama (1997), and *Protostega gigas* from Hirayama (1997). Extensive ghost lineages are shown for three taxa (*Toxochelys*, Pan-Cheloniidae, and Dermochelyidae) with the upper range for Pan-Cheloniidae shown as uncertain because of Maastrichtian and Paleocene taxa that need to be integrated into phylogenetic analyses (see Parham et al. 2014).

synapomorphies, their placement in other phylogenies has been very unstable (Joyce 2007, Danilov and Parham 2008, Rabi et al. 2013, Pérez-García et al. 2014, Zhou et al. 2014) and we caution that their exclusive monophyly could be an analytical artifact. The possibility that some of these taxa are pan-chelonioids remains to be carefully demonstrated, but it is worth noting that over the past 12 years the presence of Late Cretaceous macrobaenids in North America (Parham and Hutchison 2003, Parham 2005, Brinkman et al. 2010) puts at least some of these taxa in geographic and temporal proximity to the origin of other americhelyidan lineages.

Jurassic marine turtles have been associated with protostegids ever since Joyce (2007) placed *Sa. gaffneyi* with *So. parsonsi* and *J. oleronensis* outside of crown group Cryptodira. Our analysis retains that association by placing the Jurassic forms and protostegids into the crown group Chelonioidea, within Americhelydia. The possibility that just the protostegids are especially related to Jurassic marine turtles (*sensu* Joyce 2007) is not supported by our analysis, but is worth further consideration along with the possibility that the marine lineages that originate in the Jurassic, Early Cretaceous (protostegids), and Late Cretaceous (chelonioids) represent three or more independent radiations. Our skepticism about the cladistic pattern stems from the low statistical support for the base of Pan-Chelonioidea, as well as the lack of an evolutionary scenario that reconciles patterns of time, geography, and anatomy. We illustrate the troubling lack of consilience below.

Protostegids are the only marine turtle clade known from the Early Cretaceous; they are known from Australia (Kear and Lee 2006) and South America (Hirayama 1998, this study) and Europe (Collins 1970). The initial appearance of protostegids in southern continents (this study) is surprising because cryptodires are a largely Eurasian clade in the Early Cretaceous, and the continents that comprised Gondwana are dominated by pleurodires (Crawford et al. 2015). The oldest unanimously accepted non-protostegid chelonioid *s.l.* is *T. latiremis* from the Upper Cretaceous of North America. In addition to being temporally and geographically distant from protostegids, *T. latiremis* is the least specialized chelonioid *s.l.* (Zangerl 1953b). The primitive characters and basal position of *T. latiremis*, and other undisputed pan-chelonioids from the Upper Cretaceous of North America, are conspicuous given the highly derived and pelagic-specialized morphology of Early Cretaceous protostegids (such as *D. padillai*, and *S. gaffneyi*). Setting the geography and pelagic specializations aside, the phylogenetic position of protostegids requires ghost lineages for Pan-Cheloniidae and Pan-*Dermochelys* that encompass the better part of the Cretaceous (Fig. 12). These discrepancies are part of the reason that some authors have been open to the possibility that protostegids represent an earlier independent radiation of marine turtles (Joyce et al. 2013, Parham et al. 2014).

There are other ancillary arguments that support the hypothesis that protostegids are not chelonioids. Molecular phylogenies of extant lineages show that the non-marine lineage that is most closely related to chelonioids is Chelydroidea. Fossil chelydroids first appear in the Upper Cretaceous of North America (Joyce et al. 2013) along with *T. latiremis* and other undisputed chelonioids. Retaining protostegids in Chelonioidea requires that chelydroids remain undiscovered in Lower Cretaceous formations. Removing protostegids from the chelonioids greatly simplifies biogeographic patterns since the oldest undisputed pan-chelonioids (e.g., *Toxochelys* Cope, 1873 and *Ctenochelys* Zangerl, 1953b) are from the Upper Cretaceous of North America. Moreover, the phylogenomic results of Crawford et al. (2015) show that the internodes between clades of americhelydians are very short, suggesting a rapid appearance of chelonioids and pan-chelydroids in the Late Cretaceous. This pattern is complicated by the temporal differences noted above, and further exacerbated by the inclusion of Jurassic forms on the chelonioid stem (e.g., xinjiangchelyids, *S. parsonsi*, *J. oleronesis*).

We establish here that the inclusion of marine turtle specific characters is driving the placement of protostegids in Chelonioidea (see Phylogenetic Results). It is possible that convergent marine specializations could be overriding characters that are not obviously linked to a marine ecology. If this is the case, and protostegids are actually stem cryptodires, then we should expect them to retain some unusually plesiomorphic characters. In fact, some Early Cretaceous protostegids do show some characters that do not match those of crown group chelonioids. These characters include almost all cervical articulations procoelous, an elongated first thoracic rib (known in *S. gaffneyi*), transversal process positioned at the middle of the vertebral centrum of cervicals, and prefrontals that do not meet medially (*A. ischyros, B. suteri* [polymorphic for this taxon], *D. lowi, D. padillai, Rhinochelys* spp., and *S. gaffneyi*). These characters do not occur in chelonioids or other crown group cryptodires, but are found in Early Cretaceous stem cryptodires (e.g., sinemydids).

For all of the reasons listed above, and despite the fact that our phylogenetic analysis supports the hypothesis that *D. padillai* is the oldest chelonioid, we do not recommend that it be used as a fossil calibration for that node at this time. Fossil calibrations should be based on well-demonstrated phylogenetic conclusions (Parham et al. 2012), and whereas we feel that a monophyletic Chelonioidea *s.l.* (including protostegids

in the crown) could be correct there is considerable lingering uncertainty. A consequence of this uncertainty is that the oldest specimen we can confidently assign to Chelonioidea is the holotype of the Eocene dermochelyid *Eosphargis breineri* Nielsen, 1959 (see Joyce et al. 2013). This specimen is as young as 48.4 Ma, >75 million years younger than the material of *D. padillai*.

Oldest known marine turtle?

Desmatochelys padillai is from the upper Barremian-lower Aptian "arcillolitas abigarradas" segment of Paja Formation, making its minimum age ~120.0 Ma (Cohen et al. 2013) compared to the 92.8 Ma minimum age for *S. gaffneyi* (see Joyce et al. 2013, p. 617). Because *S. gaffneyi* was considered to be the oldest known marine turtle by some authors (Hirayama 1994, 1998) this would seemingly make *D. padillai* the oldest marine turtle (Fig. 12). However, the matter is complicated by the fact that the definition of "marine turtle" is not rigorously established. Therefore, recognizing marine turtles in the fossil record can be difficult. Extant chelonioids are obviously marine turtles because they show adaptations for a pelagic marine existence (see introduction) and are always found in marine environments. The trionychid turtle *Trionyx triunguis* Forskål, 1775 has been observed in marine environments (Taskavak and Akcinar 2009), but is primarily known from freshwater sites and is never considered a marine turtle. The emydid *Malaclemys terrapin* Schoepff, 1793 is restricted to coastal saline environments (Carr 1952), but is also not considered a marine turtle. Thus it seems that the label "marine turtle" is restricted to turtles that live in marine environments that also show morphological specializations of marine turtles such as enlarged salt glands and paddles (Hirayama 1998). These features can be difficult to ascertain in the fossil record. Some combination of these characters is necessary since freshwater turtles show the development of incipient paddles (e.g., *Carettochelys insculpta* Ramsay, 1886) and also non-marine organisms can be found fossilized in marine rocks.

Turtles from the Upper Jurassic of Europe assigned to Plesiochelyidae Rütimeyer, 1873, Eurysternidae Dollo, 1886, and Thalassemydidae Zittel, 1889 have been suggested to show evidence of some of the quintessential marine turtle characters such as large foramina interorbitale for accommodation of hypertrophied salt glands in the skull and forelimbs modified into paddles (Lapparent de Broin et al. 2001, Renous et al. 2008, Anquetin et al. 2015), although these claims require further verification. On the other side of the planet, *Neusticemys neuquina* Fernández and de la Fuente, 1988 from the Upper Jurassic (Tithonian) of Argentina, shows elongated forelimbs, however they do not match those of other marine turtles and the skull is unknown (see de la Fuente and Fernández 2011). It is likely that the Jurassic forms correspond to littoral or coastal adapted turtles as has been suggested for bothremydid pleurodires (Gaffney et al. 2006, Cadena et al. 2012), stereogenyins, a group of Cenozoic podocnemidids (Ferreira et al. 2015), sandowinids (Cretaceous-Paleogene pan-cryptodires, also found in the Paja Formation of Villa de Leyva, Colombia [Cadena in press]), and the emydid *Malaclemys terrapin* mentioned above. Potential evidence of marine adapted turtles during the Jurassic comes from trackways found in France, showing evidence of synchronous forelimb movements seen in extant chelonioids (Gaillard et al. 2003). However, the absence of fossil turtles from the same stratigraphical horizon leaves the question of the track makers identity open.

The morphology and ecology of Jurassic forms require further study, but there are sufficient data to complicate the assertion that the oldest known marine turtles are Cretaceous. Nevertheless, protostegids, such as *D. padillai*, are easily labeled as marine turtles because they share many of the morphological features of extant chelonioids and are found in rocks that were deposited in an offshore marine environment. Whereas the term "oldest marine turtle" depends very much on the concept of the term being applied, we can confidently say that *D. padillai* is the oldest, definitive, fully marine turtle known to date.

ACKNOWLEDGEMENTS

Financial support for this project was provided by the following funding organizations: Palaeontological Association (research grant, 2012), Karl Hirsch Memorial Grant, Western Interior Paleontological Society (2012), the Doris O. and Samuel P. Welles Research Fund of the University of California Museum of Paleontology (2012), Paleontological Research Institution (2012), Chicago Herpetological Society (2012), Toomey Foundation for the Natural Sciences (2012), and the Alexander von Humboldt Foundation of Germany. We thank A. Krapf (NMW), P. Holroyd (UCMP), R. Ernst (MTKD), and V. Schneider (NCSM) for help with access to specimens. Special thanks to C. B. Padilla (R.I.P), S. Padilla, M. Parra and her brothers for their amazing job at the Center of Paleontological Investigations and for allowing us access to the specimens.

LITERATURE CITED

Anquetin, J. 2012. Reassessment of the phylogenetic interrelationships of basal turtles (Testudinata). *Journal of Systematic Palaeontology* 10:3–45.

Anquetin, J., C. Püntener, and J.P. Billon-Bruyat. 2015. *Portlandemys gracilis* n. sp., a New Coastal Marine Turtle from the Late Jurassic of Porrentruy (Switzerland) and a Reconsideration of Plesiochelyid Cranial Anatomy. *PLoS ONE* 10(6):e0129193. doi:10.1371/journal.pone.0129193

Bardet, N, N.E, Jalil, F.de. Lapparent de Broin, D. Germain, O. Lambert, and M. Amaghzaz. 2013. A Giant Chelonioid Turtle from the Late Cretaceous of Morocco with a Suction Feeding Apparatus Unique among Tetrapods. *PLoS ONE* 8(7):e63586 doi:10.1371/journal.pone.0063586.

Batsch, A.J. 1788. Versuch einter Anleitung, zur Kinntniss und Geschichte der Thiere und Mineralien. *Akademische Buchhandlung*. Jena, Germany.

Baur, G. 1893. Notes on the classification of the Cryptodira. *American Naturalist* 27:672–675.

Brinkman, D.B., M.J. Densmore, and W.G. Joyce. 2010. "Macrobaenidae" (Testudines: Eucryptodira) from the Late Paleocene (Clarkforkian) of Montana and the TaxonomicTreatment of *"Clemmys" backmani*. *Bulletin of the Peabody Museum of Natural History* 51(2):147–155.

Brinkman, D.B., M. Hart, H. Jamniczky, and M. Colbert. 2006. Nichollsemys baieri gen. et. sp. nov, a primitive chelonioid turtle from the Late Campanian of North America. *Paludicola* 5:111-124.

Cadena, E.A. In press. A new pan-cryptodire (Sandownidae) turtle from the lower Cretaceous of Colombia supports the actual environmental adaptations of the group. *PeerJ*.

Cadena, E.A., J.I. Bloch, and C.A. Jaramillo. 2012. New bothremydid turtle (Testudines, Pleurodira) from the Paleocene of North-Eastern Colombia. *Journal of Paleontology* 87:686–699.

Carballido J.L., D. Pol, M.L. Parra-Ruge, S. Padilla-Bernal, M.E. Páramo-Fonseca, and F. Etayo-Serna. In press. A new Early Cretaceous brachiosaurid (Dinosauria, Neosauropoda) from northwestern Gondwana (Villa de Leiva, Colombia), *Journal of Vertebrate Paleontology*.

Carr, A. 1952. Handbook of Turtles. Cornell University Press, Ithaca, New York.

Cohen, K.M., S.M. Finney, P.L. Gibbard, and J.X, Fan. 2013. The ICS International Chronostratigraphic Chart. *Episodes* 36(3):199–204.

Collins J.I. 1970. The chelonian *Rhinochelys* Seeley from the Upper Cretaceous of England and France. *Palaeontology* 13:355–378.

Cope, E.D. 1868. On the origin of genera. *Proceedings of the Academy of Natural Sciences of Philadelphia* 20:242–300.

Cope, E.D. 1872. A description of the genus *Protostega*, a form of extinct Testudinata. *Proceedings of the American Philosophical Society* 1872:12.

Cope, E.D. 1873. *Toxochelys latiremis*. *Proceedings of the Academy of Natural Sciences of Philadelphia* 1873:10.

Crawford, N.G., J.F. Parham, A.B. Sellas, B.C. Faircloth, T.C. Glenn, T.J. Papenfuss, J.B. Henderson, M.H. Hansen, and W.B. Simison. 2015. A phylogenomic analysis of turtles. *Molecular Phylogenetics and Evolution* 83:250–257.

Danilov, I.G., and J.F. Parham. 2006. A redescription of '*Plesiochelys*' *tatsuensis*, a turtle from the Late Jurassic of China, and its bearing on the antiquity of the crown clade Cryptodira. *Journal of Vertebrate Paleontology* 26:573–580.

Danilov, I.G., and J.F. Parham. 2008. A reassessment of some poorly known turtles from the Middle Jurassic of China with comments on the antiquity of extant turtles. *Journal of Vertebrate Paleontology* 28:306–318

de la Fuente, M.S., and M.S. Fernández. 2011. An unusual pattern in the limb morphology of the Tithonian marine turtle *Neusticemys neuquina* from the Vaca Muerta Formation (Neuquén Basin) Argentina. *Lethaia* 44:5–25.

Dollo, M.L. 1886. Premiere note sur les Cheloniens du Bruxellien (kocene moyen) de la Belgique. *Bulletin Museum Royale Histoire Naturelle de Belgique* IV:79.

Dollo, M.L. 1903. *Eochelone brabantica*, tortue marine nouvelle du Bruxellien (Eocene moyen) de la Belgique. *Bulletin de la Classe des Sciences, Academie Royale de Belgique* 8:792–801.

Dornburg, A., J.M. Beaulieu, J.C. Oliver, and T.J. Near. 2011. Integrating fossil preservation bias in the selection of calibrations for molecular divergence time estimation. *Systematic Biology* 60:519–527

Elliott, D.K, G.V. Irby and J.H. Hutchison.1997. *Desmatochelys lowi*, a marine turtle from the Upper Cretaceous. Pp. 243–258 *in* J.M Callaway and E.M Nicholls (eds.), Ancient marine reptiles. Academic Press, San Diego.

Etayo-Serna, F. 1968. El sistema Cretáceo en la región de Villa de Leyva y zonas próximas. *Geología Colombiana* 5:5–74.

Etayo-Serna, F. 1979. Zonation of the Cretaceous of central Colombia by ammonites. *Publicaciones Geológicas Especiales del Ingeominas* 2:1–186.

Fernández, M.S., and M.F. de la Fuente. 1988. Una nueva tortuga (Cryptodira: Thalassemydidae) de la Formación Vaca Muerta (Jurásico: Titoniano) de la provincia del Neuquén, Argentina. *Ameghiniana* 25:129–138.

Ferreira, G.S., A.D. Rincón., A. Solórzano., and M. Langer. 2015. The last marine pelomedusoids (*Testudines*: *Pleurodira*): a new species of *Bairdemys* and the paleoecology of *Stereogenyina*. *PeerJ* 3:e1063; DOI 10.7717/peerj.1063.

Forskål, P. 1775. Descriptiones Animalium: Avium, Amphibiorum, Piscium, Insectorum, Vermium; quae in Itinere Orientali Observavit. Post mortem auctoris edidit Carsten Niebuhr. Hauniae [Copenhagen] Mölleri, 164 pp.

Gaffney, E.S. 1975. A phylogeny and classification of the higher categories of turtles. *Bulletin of the American Museum of Natural History* 155:389–436.

Gaffney, E.S., H. Tong, and P.A. Meylan. 2006. Evolution of the side-necked turtles: the families Bothremydidae, Euraxemydidae, and Araripemydidae. *Bulletin of the American Museum of Natural History* 300:1–698.

Gaillard, C., P.Bernier, G. Barale, J.P. Bourseau, E. Buffetaut, R. Ezquerra, J.C. Gall, F.de. Lapparent de Broin, S. Renous, and S. Wenz. 2005. A giant upper Jurassic turtle revealed by its trackways. *Lethatia* 36:315–322.

Hay, O.P. 1908. The Fossil Turtles of North America. Carnegie Institute of Washington, Publication Number 75, 568 p.

Hampe, O. 2005. Considerations on a *Brachauchenius* skeleton (Pliosauroidea) from the lower Paja Formation (late Barremian) of Villa de Leyva area (Colombia). *Mitten Museum Naturekunden Berlin Geowiss Reihe* 8:37–51.

Hirayama, R. 1994. Phylogenetic systematics of chelonioid sea turtles. *The Island Arc* 3:270–284.

Hirayama, R. 1997. Distribution and diversity of Cretaceous chelonioids. Pp. 225–241 *in* J.M Callaway and E.M Nicholls (eds.), Ancient marine reptiles. Academic Press, San Diego.

Hirayama, R. 1998. Oldest known sea turtle. *Nature* 392(6677):705–708.

Hirayama, R., and T. Chitoku. 1996. Family Dermochelyidae (Superfamily Chelonioidea) from the Upper Cretaceous of North Japan. *Transactions and Proceedings of the Palaeontological Society of Japan* 184:597–622.

Hirayama, R., A. Furii, and K. Takahashi. 2006. A dermochelyid sea turtle from the Upper Cretaecous (Late Campanian) Izumi Group of Shionoe, Takamatsu city, Kagawa Perfecture, Western Japan. *Fossils. The Paleontological Society of Japan* 80:17–20.

Hoedemaeker, P.J. 2004. On the Barremian-lower Albian stratigraphy of Colombia. *Scripta Geologica* 128:3–15.

Hooks, G.E. 1998. Systematic revision of the Protostegidae, with a redescription of *Calcarichelys gemma* Zangerl, 1953. *Journal of Vertebrate Paleontology* 18(1):85–98.

Jones, M.E., I. Werneburg, N. Curtis, R. Penrose, P. O'Higgins, M.J. Fagan, and S.E Evans. 2013. The Head and Neck Anatomy of Sea Turtles (Cryptodira: Chelonioidea) and Skull Shape in Testudines. *PLoS ONE* 7(11):e47852. doi:10.1371/journal.pone.0047852.

Joyce, W.G. 2000. The first complete skeleton of *Solnhofia parsonsi* (Cryptodira, Eurysternidae) from the Upper Jurassic of Germany and its taxonomic implications. *Journal of Paleontology* 74:684–700.

Joyce, W.G. 2007. Phylogenetic relationships of Mesozoic Turtles. *Bulletin of Peabody Museum of Natural History* 48(1):3–102.

Joyce, W.G., S.D. Chapman, R.T.J. Moody, and C.A. Walker. 2011. The skull of the solemydid turtle *Helochelydra nopcsai* from the Early Cretaceous of the Isle of Wight (UK) and a review of Solemydidae. *Special Papers in Palaeontology* 86:75–97.

Joyce, W.G., J.F. Parham, and J.A. Gauthier. 2004. Developing a protocol for the conversion of rank-based taxon names to phylogenetically defined clade names, as exemplified by turtles. *Journal of Paleontology* 78:989–1013.

Joyce, W.G., J.F. Parham, T.R. Lyson, R.C.M. Warnock, and P.C.J. Donoghue. 2013. A divergence dating analysis of turtles using fossil calibrations: an example of best practices. *Journal of Paleontology* 87:612–634.

Kear, B.P., and M.S.Y. Lee. 2006. A primitive protostegid from Australia and early sea turtle evolution. *Biology Letters* 2:116–119.

Khosatzky, L.I., and M. Mlynarski. 1971. Chelonians from the upper Cretaceous of the Gobi Desert, Mongolia. *Paleontologica Polonica* 25:131–144.

Knauss, G., W.G. Joyce, T.R. Lyson, and D. Pearson. 2011. A new kinosternoid from the Late Cretaceous Hell Creek Formation of North Dakota and Montana and the origin of the *Dermatemys mawii* lineage. *Paläontologische Zeitschrift* 85:125–142.

Lapparent de Broin, F. de. 2001. The European turtle fauna from the Triassic to the present. *Dumerilia* 4:155–216.

Lapparent de Broin, F. de, X. Murelaga, F. Farrés, and J. Altimiras. 2014a. An exceptional cheloniid turtle, *Osonachelus decorata* nov. gen., nov. sp., from the Eocene (Bartonian) of Catalonia (Spain). *Geobios* 47:111–132.

Lapparent de Broin, F. de, N. Bardet, M. Amaghzaz, and S. Meslouh. 2014b. A strange new chelonioid turtle from the Latest Cretaceous Phosphates of Morocco. *Comptes Rendus Palevol* 13(2):87–95.

Lehman, T.M., and S.L. Tomlinson. 2004. *Terlinguachelys fischbecki*, a new genus and species of sea turtle (Chelonioidea: Protostegidae) from the upper Cretaceous of Texas. *Journal of Paleontology* 78(6):1163–1178.

Linnaeus, C. 1758. Systema Naturae, Volume 1 (10th edition). Laurentius Salvius, Holmia, 824p.

Maddison, W.P., and D.R. Maddison. 2009. Mesquite: a modular system for evolutionary analysis. Version 3.01 [updated at http://mesquiteproject.org].

Marshall, C.R. 2008. A simple method for bracketing absolute divergence times on molecular phylogenies using multiple fossil calibration points. *American Naturalist* 171:726–742.

Martill, D.M. 2007. The age of the Cretaceous Santana Formation fossil Konservat Lagerstätte of north-east Brazil: a historical review and an appraisal of the biochronostratigraphic utility of its palaeobiota. *Cretaceous Research* 28:895–920.

Moody, R.T.J. 1974. The taxonomy and morphology of *Puppigerus camperi* (Gray), an Eocene sea-turtle from northern Europe. *Bulletin of the British Museum (Natural History) Geology* 25:153–186.

Near, T.J., P.A. Meylan. and H.B. Shaffer. 2005. Assessing concordance of fossil calibration points in molecular clock studies: An example using turtles. *American Naturalist* 165:137–146.

Near, T.J., P.A. Meylan, and H.B. Shaffer. 2008. Caveats on the use of fossil calibrations for molecular dating: a reply to Parham and Irmis. *American Naturalist* 171:137–140.

Nessov, L.A. 1990. Xinjiangchelyidae. Pp 185–204 *in* M.N. Kaznyshkin, L.A. Nalbandyan and L.A. Nessov. Turtles of middle and late Jurassic of Fergana (Kirghiz SSR)," Ezhegod. Vsesoyuz. *Paleontologicheskogo Obshchestva* 33.

Nicholls, E.L. 1992. Note on the occurrence of the marine turtle *Desmatochelys* (Reptilia:Chelonioidea) from the Upper Cretaceous of Vancouver Island. *Canadian Journal of Earth Sciences* 29:377–380.

Nielsen, E. 1959. Eocene turtles from Denmark. Medd. Fra Dansk Gel. F. Bd. 14 part 2. 120 Pp.

Oppel, M. 1811. Die Ordnungen, Familien und gattungen der reptilien als prodrom einer Naturgeschichte derselben. J. Lindauer, München, pp. i–xii, 1–86.

Owen, R. 1842. Report on the British reptiles. *Report of the British Association for the Advancement of Science* 1841:60–204.

Padilla, C.B. 2011. Classic and recent methods using acids in preparation. II Conservation Workshop, Barcelona, Spain pp 2–10.

Parham, J.F. 2005. A reassessment of the referral of sea turtle skulls to the genus *Osteopygis* (Late Cretaceous, New Jersey, USA). *Journal of Vertebrate Paleontology* 25:71–77.

Parham, J.F., P.C.J. Donoghue, C.J. Bell, T.D. Calway, J.J. Head, P.A. Holroyd, J.G. Inoue, R.B. Irmis, W.G. Joyce, D.T. Ksepka, J.S.L. Patané, N.D. Smith, J.E. Tarver, M. Van Tuinen, Z. Yang, K.D. Angielczyk, J. Greenwood, C.A. Hipsley, L. Jacobs, P.J. Makovicky, J. Müller, K.T. Smith, J.M. Theodor, R.C.M. Warnock, and M.J. Benton. 2012. Best practices for justifying fossil calibrations. Systematic Biology 61(2):346-359.

Parham, J.F., and J.H. Hutchison. 2003. A new eucryptodiran turtle from the Late Cretaceous of North America (Dinosaur Provincial Park, Alberta, Canada). *Journal of Vertebrate Paleontology* 23:783–798.

Parham, J.F., and R.B. Irmis. 2008. Caveats on the use of fossil calibrations for molecular dating. *American Naturalist* 171:132–136.

Parham, J.F., R.A. Otero, and M.E. Suárez. 2014. A sea turtle skull from the Cretaceous of Chile with comments on the taxonomy and biogeography of *Euclastes* (formerly *Osteopygis*). *Cretaceous Research* 49: 181–189.

Parham, J.F., and N.D. Pyenson. 2010. New sea turtle from the Miocene of Peru and the iterative evolution of feeding ecomorphologies since the Cretaceous. *Journal of Paleontology* 84: 231–247.

Patarroyo, P. 2000. Distribución de ammonitas del Barremiano de la Formación Paja en el sector de Villa de Leyva (Boyacá, Colombia). Bioestratigrafía. *Geología Colombiana* 25:149–162.

Patarroyo, P. 2004. Die Entwicklung der Ammoniten der Familie Pulchelliidae aus dem Barrême von Zentral-Kolumbien. *Revue de Paléobiologie* 23:1–65.

Pérez-García, A. 2015. New data on the poorly-known Late Jurassic European turtles *Thalassemys* and *Enaliochelys* and description of a new basal eucryptodiran taxon. *Journal of Iberian Geology* 41(1):21–30.

Pérez-García, A., J.M. Gasulla, and F. Ortega. 2014. A new species of *Brodiechelys* (Testudines, Pan-Cryptodira) from the Early Cretaceous of Spain: Systematic and palaeobiogeographic implications. *Acta Palaeontologica Polonica* 59:333–342.

Pyenson, N.D., N.P. Kelley and J.F. Parham. 2014. Marine tetrapod macroevolution: Physical and biological drivers on 250 Ma of invasions and evolution in ocean ecosystems. *Palaeogeography, Palaeoclimatology, Palaeoecology* 400:1–8.

Rabi, M., V.B. Sukhanov, V.N. Egorova, and I. Danilov. 2014. Osteology, relationships, and ecology of *Annemys* (Testudines, Eucryptodira) from the late Juassic of Shar Teg, Mongolia, and phylogenetic definitions for Xinjiangchelyidae, Sinemydidae, and Macrobaenidae. *Journal of Vertebrate Paleontology* 34(2):327–352.

Rabi, M., C.F. Zhou, O. Wings, S. Ge, and W.G. Joyce. 2013. A new xinjiangchelyid turtle from the Middle Jurassic of Xinjiang, China and the evolution of the basipterygoid process in Mesozoic turtles. *BMC Evolutionary Biology* 13:203.

Ramsay, E.P. 1886. On a new genus and species of fresh water tortoise from the Fly River, New Guinea. *Proceedings of the Linnaean Society of New South Wales* 2(1):158–162.

Renous, S., F. de Lapparent de Broin, M. Depecker, J. Davenport, and V. Bels. 2008. Evolution of locomotion in aquatic turtles. Pp 97–138 *in* J. Wyneken, V. Bels and M. H. Godfrey (Eds.), Biology of turtles, CRC press, Boca Raton.

Rütimeyer, L. 1873. Die fossilen Schildkröten von Solothurn. *Neue Denkschrift der Allgemeinen Schweizerischen Naturforschenden Gesellschaft* 25:1–185.

Schoepff, J.D. 1793. Historia Testudinum iconibus illustrata. Erlangae: *Ioannis Iacobi Palm* 136:33–80.

Seeley, H.G. 1869. Index to the fossil remains Aves, Ornithosauria and Reptilia from the Secondary System of strata arrange in the Woodwardian Museum of the University of Cambridge. Cambridge Universty Press. 100 pp.

Smith, D.T.J. 1989. The cranial morphology of fossil and living sea turtles (Cheloniidae, Dermochelyidae and Desmatochelyidae). Ph.D. thesis, Kingston Polytechnic, Surrey, England, 310 pp.

Springer, M.S., E.C. Teeling, O. Madsen, M.J. Stanhope, and W.W. de Jong. 2001. Integrated fossil and molecular data reconstruct bat echolocation. *Proceedings of the National Academy of Science* 98:6241–6246.

Sterli, J. 2008. A new, nearly complete stem turtle from the Jurassic of South America with implications for turtle evolution. *Biology Letters* 4:286–289.

Sterli, J., 2010. Phylogenetic relationships among extinct and extant turtles: the position of Pleurodira and the effects of the fossils on rooting crown-group turtles. Contrib. Zool. 79, 93–106.

Sterli, J., and M.S. de la Fuente. 2013. New evidence from the Palaeocene of Patagonia (Argentina) on the evolution and palaeo-biogeography of Meiolaniformes (Testudinata, new taxon name). *Journal of Systematic Palaeontology* 11(7):835–852.

Sukhanov, B. 1964. Subclass Testudinata. Pp. 354–438 *in* Y.A. Orlov (ed.) Osnovy paleontologii. Zemnovodnye, presmykayushchiesya i ptitsy. Nauka, Moscow.

Swofford, D. 2002. PAUP*. Phylogenetic Analysis Using Parsimony (*and other methods). Version 4.0b10. Sinauer Associates, Sunderland.

Taskavak, E., and S.C. Akcinar. 2009. Marine records of the Nile soft-shelled turtle, *Trionyx triunguis* from Turkey. *Marine Biodiversity Records* 2:1–4.

Tatarinov, L.P. 1959. A new turtle of the family Baenidae from the Lower Eocene of Mongolia. *Paleontologicheskii Zhurnal* 1:100–113.

Tong, H., R. Hirayama, E. Makhoul, and F. Escuillie. 2006. *Rhinochelys* (Chelonioidea: Protostegidae) from the Late Cretaceous (Cenomanian) of Nammoura, Lebanon. *Atti Soc It Sci nat Museo civ Stor nat Milano* 147(1):113–138.

Vandellius, D. 1761. Epistola de holothurio, et *testudine coriacea* ad celeberrimum Carolum Linnaeum equitem naturae curiosorum dioscoridem II. Padua (Conzatti), 12 S.

Vandermark, D., J.A. Tarduno, D.B. Brinkman, R.D. Cottrell, and S. Mason. 2009. New Late Cretaceous macrobaenid turtle with Asian affinities from the High Canadian Arctic: Dispersal via ice-free polar routes. *Geology* 37:183–186

Warnock, R.C.M., J.F. Parham, W.G. Joyce, T.R. Lyson, and P.C.J. Donoghue. 2015. Calibration uncertainty in molecular dating analyses: there is no substitute for the prior evaluation of time priors. *Proceedings of the Royal Society B* 282:20141013.

Wieland, G.R. 1896. *Archelon ischyros*: a new gigantic cryptodire testudinate from the Pierre Cretaceous of South Dakota. *American Journal of Science* 4:95–108.

Williston, S.W. 1894. A new turtle from the Benton Cretaceous. *Kansas University Quarterly* 3:5–18.

Wiman, C. 1963. Fossile Schildkröten aus China. *Paleontologica Sinica* 6:1–56.

Yeh, X. 1963. Fossil turtles from China. *Palaeontologica Sinica* 18:1–112.

Yeh, X. 1986. A Jurassic turtle from Junggar, Xinjiang. *Vertebrata PalAsiatica* 24:171– 181.

Zangerl, R. 1953a. The Vertebrate Fauna of the Selma Formation of Alabama. Part III. The turtles of the family Protostegidae. *Fieldiana Geology* 3:59–133.

Zangerl, R. 1953b. The vertebrate fauna of the Selma Formation of Alabama. Part IV. The turtles of the family Toxochelyidae. *Fieldiana Geology* 3:135–277.

Zangerl, R., and Sloan R.E. 1960. A new specimen of *Desmatochelys lowi* Williston, a primitive cheloniid sea turtle from the Cretaceous of South Dakota. *Fieldiana Geology* 14:7–40.

Zhou, C-F., M. Rabi, and W.G. Joyce. 2014. A new specimen of *Manchurochelys manchoukuoensis* from the Early Cretaceous Jehol Biota of Chifeng, Inner Mongolia, China and the phylogeny of Cretaceous basal eucryptodiran turtles. *BMC Evolutionary Biology* 14:77.

Zittel, K.A. 1889. Handbuch der Palaeontologie. Section 1: Palaeozoologie, Volume 3, Vertebrata, Shipment 3: Reptilia. München: R. Oldenbourg.

SUPPLEMENTARY INFORMATION 1

List of characters used in this study. Authors abbreviations: AN, Anquetin (2012); BR, Bardet et al. (2013); HY1, Hirayama (1994); HY2, Hirayama (1998); JY1, Joyce (2007); JY2, Joyce et al. (2011); KL, Kear and Lee (2006); PH, Parham and Pyenson (2010); ST, Sterli (2008); STF, Sterli and de la Fuente (2013). See the respective reference for discussion, previous references or history of the character. Recent changes to characters numbers from HY2 original matrix can be found in Lapparent de Broin et al. (2014a). The final Mesquite matrix can be downloaded at http://escholarship.org/uc/item/147611bv/27300-106320-15-ED.txt.

Skull

1. Nasals: 0 = present; 1 = absent. JY1 & STF (ch 1, Nasal A). HY2, KL, BR (ch 2).
2. Nasals, medial contact of nasals: 0 = nasals contact one another medially along their entire length; 1 = medial contact of nasals partially or fully hindered by long anterior frontal process. JY1 & STF (ch 2, Nasal B).
3. Nasals, size of nasals: 0 = dorsal exposure of nasals large; 1 = dorsal exposure of nasals greatly reduced relative to that of the frontals. JY1 & STF (ch 3, Nasal C).
4. Prefrontals, medial contact of prefrontals on the dorsal skull surface: 0 = absent; 1 = present, absence of contact between the nasal or apertura narium externa and the frontal. JY1 & STF (ch 4, Prefrontal A), HY2, KL, BR (ch 3).
5. Prefrontals, prefrontal-vomer contact: 0 = present; 1 = absent. JY1 & STF (ch 5, Prefrontal B).
6. Prefrontals, prefrontal-palatine contact: 0 = present; 1 = absent. JY1 & STF (ch 6, Prefrontal C).
7. Prefrontals, dorsal prefrontal exposure: 0 = present, large; 1 = reduced; 2 = absent or near absent. JY1 & STF (ch 7, Prefrontal D). Remarks: Anquetin (2012) splits this character in two: AN (ch 9) & (ch 10) arguing for a better test of the congruence of the lack of a dorsal exposure of prefrontals in the phylogenetic analysis. Ordered.
8. Prefrontals, cranial scutes on the prefrontal: 0 = one pair; 1 = two pairs or more. PH (ch 10); HY2 & KL (ch 1); BR (ch 1). Remarks: State 1 modified considering the presence of more than two pairs of scutes in *Eretmochelys imbricata* and *Lepidochelys kempii*.
9. Lacrimal: 0 = present; 1 = absent. JY1 & STF (ch 9, Lacrimal A).
10. Frontals, frontal contribution to orbit: 0 = absent, contact between prefrontal and postorbital; 1 = present. JY1 & STF (ch 10, Frontal A); HY2 & KL (ch 4); BR (ch 4), reversing polarity of HY (ch 4) to (0: present, 1: absent). Remarks: Sterli and de la Fuente (2013) coded *Caretta caretta* as 0&1, but after direct examination of important number of extant specimens all have state 0 (see Table 1S).
11. Frontals, both frontals medially fused: 0 = absent; 1 = present. Bona and de la Fuente (2005) and STF (ch 11, Frontal B).
12. Frontals, direction of the orbits in dorsal view of the skull: 0 = laterally facing, with a very narrow to almost complete absent dorsal exposure of the maxilla and jugal; 1 = dorsolateral facing, with portions of the maxilla and jugal dorsally exposed. Modified from PH (ch 12); HY2, KL, BR (ch 5).
13. Parietals, parietal-squamosal contact: 0 = present, upper temporal emargination absent or poorly developed; 1 = absent, upper temporal emargination well developed. JY1 (ch 11) & STF (ch 12) (Parietal A); HY2, KL, BR (ch 7). Remarks: *Ocepechelon* and *Archelon* have a very narrow contact. Also the outline in *Alienochelys* is not complete and a very narrow contact could also be possible.
14. Parietals, closure of foramen nervi trigemini and the length of the anterior extension of the lateral braincase wall: 0 = foramen nervi trigemini anteriorly open, anterior extension of lateral braincase wall absent; 1 = foramen nervi trigemini anteriorly closed, processus inferior parietalis only produces a narrow strut anterior to the foramen nervi trigemini, usually absence of contact with palatine; 2 = foramen nerivi trigemini anteriorly closed, processus inferior parietalis produces an extended process anterior to the foramen nervi trigemini, contact with palatine commonly present. The character states of JY1 (ch 12) & STF (ch 13) (Parietal B) and JY1 (ch 13) & STF (ch 14) (Parietal C); HY2, KL, & BR (ch 6) form a logical morphocline and we therefore combine them into a single multistate character. Remarks: coded for few fossils because: poorly described specimens, lack of figures detailing this feature, or obscured by rock matrix.
15. Parietals, posterodorsal margin of the temporal fossa roofed by an overhanging process of the skull roof: 0 = absent; 1 = present. JY2 (ch 14) & STF (ch 15) (Parietal D).
16. Parietals, contribution to the processus trochlearis oticum: 0 = absent; 1 = present. Meylan and Gaffney (1989), STF (ch 17, Parietal F).
17. Parietals, foramen stapedio-temporalis: 0 = absent or weak, foramen stapedio-temporale concealed in dorsal

view; 1 = moderate foramen stapedio-temporale, partial exposition of the processes trochlearis in dorsal view; 2 = strong, entire exposition of the processus trochlearis in dorsal view. STF (ch 19, Parietal H). Ordered.

18. Parietals, pineal foramen located medially between parietals: 0 = absent; 1 = present. New character.
19. Jugals, jugal-squamosal contact: 0 = present; 1 = absent, contact between postorbital and quadratojugal present. JY1 (ch 14) & STF (ch 20) (Jugal A); HY1 (ch 8).
20. Jugals, jugal participation in the rim of the upper temporal emargination: 0 = absent; 1 = present, upper temporal emargination extensive. JY1 (ch 15) & STF (ch 21) (Jugal B).
21. Jugals, jugal-quadrate contact: 0= absent; 1= present, quadratojugal does not contribute to lower temporal margin. HY2, KL & BR (ch 9).
22. Jugals, medial process of jugal beneath orbit, seen in ventral view to slightly ventroposterior view: 0 = weakly developed or absent, jugal only contacts the maxilla; 1 = weak to moderately developed, presence of a contact between the jugal and pteygoid due to the lateral extension of this last; 2 = strongly developed, jugal contacts the pterygoid, the palatine, and the maxilla. Combined and modified from HY2, KL & BR (ch 10 and ch 11). Remarks: Ventral view is not always precise enough to see the contact, so there might be some specimens for which there is a contact between the palatine and the jugal but it is slightly or completely hidden by the maxilla or the palatine, that is why we included the observation of ventroposterior view of the skull in the definition of this character. Ordered.
23. Quadratojugals, deep lower temporal emargination extending above the upper limit of the cavum tympani and the resulting loss of the quadratojugal: 0 = absent; 1 = present. Reworded from JY1 (ch 16) & STF (ch 22) (Quadratojugal A) and AN (ch 22); HY2, KL & BR (ch 12).
24. Quadratojugals, quadratojugal-maxilla contact: 0 = absent; 1 = present, jugal does not contribute to lower temporal emargination. JY1 (ch 17) & STF (ch 23) (Quadratojugal B).
25. Quadratojugals, quadratojugal-squamosal contact below the cavum tympani: 0 = absent; 1 = present. JY2 (ch 19) & STF (ch 24) (Quadratojugal C) and AN (ch 24).
26. Squamosals, squamosal-postorbital contact: 0 = present; 1 = absent, temporal roofing well developed, but postorbital short; 2 = absent, due to lower temporal emargination; 3 = absent, due to upper temporal emargination. JY1 (ch 18) & STF (ch 25) (Squamosal A). Remarks: Anquetin (2012) omitted this character, however we do not share his concerns in regard to this character and maintain it as developed by Joyce (2007).
27. Squamosals, squamosal-supraoccipital contact: 0 = absent; 1 = present. JY1 (ch 19) & STF (ch 26) (Squamosal B).
28. Squamosals, posterolateral protuberances developing horns: 0 = absent; 1 = present. Gaffney (1996), STF (ch 27, Squamosal C).
29. Squamosals, very long posterior process, formed exclusively by the squamosal and protruding beyond condyles occipitalis: 0 = absent; 1 = present. Gaffney et al. (2006) & STF (ch 28, Squamosal D).
30. Squamosals, squamosal-quadrate contact: 0 = tightly sutured; 1 = wide open. STF (ch 29, Squamosal E).
31. Postorbitals, postorbital-palatine contact: 0 = absent; 1 = present, foramen palatinum posterius situated posterior to the orbital wall. JY1 (ch 20) & STF (ch 30) (Postorbital A).
32. Supratemporal: 0 = present; 1 = absent. JY1 (ch 21) & STF (ch 31) (Supratemporal A).
33. Premaxilla, subdivision of the apertura narium externa by an internarial process of the premaxilla only: 0 = present; 1 = absent. JY2 (ch 24) & STF (ch 32) (Premaxilla A).
34. Premaxilla, fusion of premaxillae: 0 = absent; 1 = present. JY1 (ch 23) & STF (ch 33) (Premaxilla B).
35. Premaxilla, foramen praepalatinum: 0 = present; 1 = absent; 2 = absent, foramen intermaxillaris present. JY1 (ch 24) & STF (ch 34) (Premaxilla C); HY2, KL & BR (ch 14). Anquetin (2012) modified this character from multistate to binary, however we do not follow the logic of Anquetin and maintain it as developed by Joyce (2007).
36. Premaxilla, exclusion of the premaxillae from the apertura narium externa: 0 = absent; 1 = present. JY1 (ch 25) & STF (ch 35) (Premaxilla D).
37. Premaxilla, distinct, medial premaxillary hook along the labial margin of the premaxillae: 0 = absent; 1 = present. JY1 (ch 26) & STF (ch 36) (Premaxilla E); HY2, KL & BR (ch 13).
38. Palatines, palatine contribution to the anterior extension of the lateral braincase wall: 0 = absent; 1 = present, well-developed. JY1 (ch 30) & STF (ch 48) (Palatine A).
39. Palatines, contribution to the upper triturating surface: 0 = absent or less than 30% of the total width of the triturating surface; 1 = present, at least 30% or more of the total width of the triturating surface. Modified from HY2, KL, BR (ch 15), STF (ch 38, Maxilla B).
40. Palatines, secondary palate: 0 = absent; 1 = present, complete separation of the narial cavity from the oral cavity. PH (ch 1); BR (ch 15) & STF (ch 39, Maxilla C).

41. Palatines, vomer-palatine contact anterior to internal naris (apertura narium interna): 0 = absent; 1 = present. HY2, KL, & BR (ch 18). Remarks: Character visible in ventral/palatal view.
42. Maxilla, triturating surface definition: 0 = triturating surface with labial ridge only; 1 = triturating surface with labial and lingual ridge; 2 = triturating surface with labial, lingual, and accessory ridge(s). AN (ch 38); HY2, KL, & BR (ch 19); STF (ch 40, Maxilla D). Remarks: Sterli and de la Fuente (2013) coded *Chelydra serpentina* and *Caretta caretta* as lacking a lingual ridge (0), but the lingual ridge is present in both taxa, coded here as (1). Ordered.
43. Maxilla, accessory ridge(s): 0 = accessory ridge(s) on maxilla present along the triturating surface; 1 = accessory ridge(s) only in some sectors of the triturating surface. Gaffney (1992); STF (ch 41, Maxilla E).
44. Vomer, number of vomer(s): 0 = paired; 1 = single, but large; 2 = single and greatly reduced or absent. JY1 (ch 26) & STF (ch 42) (Vomer). Remarks: Anquetin (2012) split the character in two AN (ch 41 and ch 42), however we prefer to keep this character as unique and multistate.
45. Vomer, vomer-pterygoid contact in palatal view: 0 = present; 1 = absent, medial contact of palatines present. JY1 (ch 28) & STF (ch 43) (Vomer B); HY2, KL & BR (ch 20).
46. Vomer, vomerine and palatine teeth: 0 = present; 1 = absent. JY1 (ch 29) & STF (ch 44) (Vomer C).
47. Vomer, vomer-premaxilla contact in ventral view: 0 = broad, anterior margin of the vomer straight; 1 = very reduced, anterior margin of vomer forming an acute tip; 2 = absent, both maxilla meeting medially. ST (ch 31); PH (ch 4 and ch 9); STF (ch 45, Vomer D). Remarks: *Chelonia mydas* is coded here as (0) after direct examination of specimens (see Table 1S). This character strictly deals with the contact on ventral surface of the skull; a premaxilla-vomer contact can be absent in ventral view but present dorsoanteriorly inside the palate. Ordered.
48. Vomer, ventral crest: 0 = absent; 1 = narrow and tall ventral crest present all along the vomer. Reworded from STF (ch 46, Vomer E).
49. Vomer, shape of the palate roof: 0 = flat; 1 = domed. Reworded from Gaffney (1983) and STF (ch 47, Vomer F). Remarks: coded for few fossils because: poorly described specimens, lack of figures detailing this feature, or obscured by rock matrix.
50. Vomer, vomerine pillar visible in ventral view: 0 = vomerine pillar absent; 1 = present; 2 = present but obscured in ventral view by the posterior extension of the triturating surface of the vomer. Modified from PH (ch 2); HY2, KL, & BR (ch 17). Remarks: An additional state was added for the absence of the pillar. Ordered.
51. Vomer, contribution to the upper triturating surface; 0 = absent, triturating surface narrow to absent; 1 = present. HY2, KL, & BR (ch 16).
52. Quadrates, flooring of cavum acustico-jugulare and recessus scale tympani: 0 = absent; 1 = fully or partially present, produced by the posterior process of the pterygoid, but the pterygoid does not cover the prootic; 2 = produced by the posterior process of the pterygoid, and the pterygoid covers the prootic; 3 = fully or partially present, produced by the ventral process of the quadrate or the prootic, or both. JY1 (ch 31) & STF (ch 49) (Quadrate A). Remarks: Anquetin (2012) redefined this character to make binary, however we to keep this character as multistate defined by Joyce (2007).
53. Quadrates, development of the cavum tympani: 0 = shallow, but not developed anteroposteriorly; 1 = shallow, but anteroposteriorly developed; 2 = deep and anteroposteriorly developed. JY1 (ch 32 and ch 33, Quadrate B and C), STF (ch 50, Quadrate B+C). Ordered.
54. Quadrates, precolumellar fossa: 0 = absent; 1 = present. JY1 (ch 34) & STF (ch 51) (Quadrate D).
55. Quadrates, antrum postoticum: 0 = absent; 1 = present, quadrate does not fully enclose the anterior perimeter of the antrum; 2 = present, quadrate fully encloses the anterior perimeter of the antrum. JY1 (ch 35, Quadrate E), STF (ch 53, Antrum postoticum A). Remarks: we do not follow Sterli (2008) or Anquetin (2012) and retain this character as originally worded by Joyce (2007). Ordered.
56. Quadrates, arrangement between the quadrate, opisthotic, stapes and Eustachian tube: 0 = the quadrate and the opisthotic form an angle of 90 degrees in lateral view; 1 = present, but the quadrate and the opisthotic form an angle less than 90 degrees in lateral view; 2 = the quadrate is well developed posteroventrally enclosing only the stapes; 3 = the quadrate is well developed posteroventrally enclosing the stapes and the Eustachian tube; 4 = the quadrate enclosing stapes and the Eustachian tube helped by the posteroventral projection of the squamosal and posterior of the quadratojugal. Modified from JY2 (ch 37) & STF (ch 53) (Quadrate F). Remarks: we don't follow the rationale of Anquetin (2012) against the usage of multistate characters and recombine Anquetin's characters 52, 53, and 54 back into one multistate character, as was done by Joyce

(2007) and Sterli (2008). We furthermore do not follow Anquetin's (2012) rationale in regards to the scoring of *Meiolania platyceps*, as this taxon is similar to pleurodires in that the incisura is not close by the quadrate itself, but rather more superficially by the squamosal, postorbital, and quadratojugal. We nevertheless accept Anquetin (2012) adjustment of Joyce (2007) scoring for *Dinochelys whitei*.

57. Quadrate, processus trochlearis oticum: 0 = absent; 1 = present, very reduce; 2 = present, large forming a well defined musculatory facet. Modified from STF (ch 54, Quadrate G). Remarks: a third state is added here for those turtles with a very large processus trochlearis oticum. Ordered.
58. Quadrate, contribution to the musculatory facet of the processus trochlearis oticum: 0 = extensive contribution; 1 = small contribution, facet formed principally by the protic and/or parietal. Reworded from Meylan (1987) and STF (ch 55, Quadrate H).
59. Quadrate, qudrate-basiphenoid contact: 0 = absent; 1 = present. Lapparent de Broin and Werner (1998); Gaffney et al. (2006) (ch 104); STF (ch 56, Quadrate I).
60. Epipterygoids: 0 = present, rod like; 1 = present, laminar; 2 = absent. JY2 (ch 37) & STF (ch 57) (Epipterygoid A). Remarks: coded for few fossils because: poorly described specimens, lack of figures detailing this feature, or obscured by rock matrix.
61. Pterygoids, pterygoid teeth: 0 = present; 1 = absent. JY1 (ch 38) & STF (ch 58) (Pterygoid A).
62. Pterygoids, basipterygoid process and basipterygoid articulation: 0 = basipterygoid process present with a movable basiptergoid articulation; 1 = basipterygoid process present with a sutured basipterygoid articulation; 2 = basipterygoid process absent and sutured basipterygoid articulation. ST (ch 41), STF (ch 59, Pterygoid B). Remarks: coded for few fossils because: poorly described specimens, lack of figures detailing this feature, or obscured by rock matrix.
63. Pterygoids, interpterygoid vacuity: 0 = triangular in shape; 1 = reduced to an interpterygoid slit; 2 = reduced to a paired foramen caroticum laterale. JY1 (ch 40) & STF (ch 60) (Pterygoid C). Remarks: coded for few fossils because: poorly described specimens, lack of figures detailing this feature, or obscured by rock matrix. Ordered.
64. Pterygoids, pterygoid-basioccipital contact: 0 = absent; 1 = present. JY1 (ch 41) & STF (ch 62) (Pterygoid D).
65. Pterygoids, processus trochelaris pterygoideus: 0 = absent; 1 = present. JY1 (ch 42) & STF (ch 63) (Pterygoid E).
66. Pterygoids, foramen palatinum posterius: 0 = present; 1 = present, but open laterally; 2 = absent. JY1 (ch 43) & STF (ch 64) (Pterygoid F); HY2, KL, & BR (ch 21). Remarks: we do not follow the rationale of Anquetin (2012) against the usage of multistate characters and retain this as a multistate character. We nevertheless accept Anquetin (2012) adjustment of Joyce (2007) scoring for *Sandownia harrisi*. Ordered.
67. Pterygoids, medial contact of pterygoid: 0 = present, pterygoids in a very long medial contact with one another, longer than the basisphenoid total length in midline; 1 = present, pterygoids in medial contact with one another, contact length equal or shorter than the basisphenoid total length in midline; 2 = absent, contact of the basisphenoid with the vomer and/or palatines present. Modified from JY1 (ch 44) & STF (ch 65) (Pterygoid G). Remarks: two additional states were added to differentiate the length of the contact in relationship to the basisphenoid midline length. Ordered.
68. Pterygoids, pterygoid contribution to foramen palatinum posterius: 0 = present; 1 = absent. JY1 (ch 45) & STF (ch 66) (Pterygoid H).
69. Pterygoids, vertical flange on processus pterygoideus externus: 0 = absent; 1 = present. Zhou et al. (2014) & JY1 (ch 67) (Pterygoid I).
70. Pterygoids, contact with the exoccipital: 0 = absent; 1 = present. STF (ch 68, Pterygoid J).
71. Pterygoids, fossa podocnemidoidea or cavum pterygoidei: 0 = absent; 1 = present. Lapparent de Broin (2000); STF (ch 69, Pterygoid K).
72. Pterygoids, processus pterygoideus externus: 0 = large, forming an extensive lateral wing; 1 = reduced, forming an acute tip; 2 = extremely reduced due to the posterolateral projection of the pterygoid; 3 = absent. Modified from PH (ch 11); HY2, KL, & BR (ch 22); STF (ch 70, Pterygoid L). Ordered.
73. Pterygoids, level of the position of the pterygoid respect to basisphenoid: 0 = both bones are at the same level on ventral surface; 1 = two different levels, creating a step between the two bones. Reworded from STF (ch 71, Pterygoid M).
74. Pterygoids, medial ridge: 0 = incipient to absent; 1 = present, ridge spans nearly the full length of the pteygoids, sometimes reaching the most posterior portion of the vomer. The medial ridge is produced by the extremely concave posterolateral portions of both pterygoids. Reworded from PH (ch 14); HY2, KL, & BR (ch 23).
75. Pterygoids, extending laterally almost reaching the mandibular condyle facet: 0 = absent; 1 = present, the

pterygoid contacts the medial edge of the mandibular condyle when is seem in ventral view; 2 = present, the pterygoids extends not only laterally to reach the outline of the mandibular condyle facet, but also posteriorly far from the level of the condyles. Reworded from HY2, KL, & BR (ch 24). Ordered.

76. Supraoccipitals, crista supraoccipitalis: 0 = poorly developed; 1 = protruding significantly posterior to the foramen magnum. JY1 (ch 46) & STF (ch 72) (Supraoccipital A); HY2, KL, & BR (ch 28).
77. Supraoccipitals, large supraoccipital exposure on dorsal skull roof: 0 = absent; 1 = present. JY2 (ch 49) & STF (ch 73) (Supraoccipital B).
78. Supraoccipitals, horizontal crest in the crista supraoccipitalis: 0 = absent or poorly developed anteriorly; 1 = present, along the entire crista supraoccipitalis. STF (ch 74, Supraoccipital C).
79. Exoccipitals, medial contact of exoccipitals dorsal to foramen magnum: 0 = absent; 1 = present. JY1 (ch 48) & STF (ch 75) (Exoccipital A).
80. Basioccipital, morphology of the anteriormost part of the basioccipital: 0 = with two or one ventral tubercle; 1 = tubercle absent. ST (ch 52); STF (ch 76, Basioccipital A).
81. Basioccipital, deep C-shaped concavity between basioccipital tubera: 0 = absent; 1 = present. STF (ch 77, Basioccipital B).
82. Prootic, dorsal exposure: 0 = large; 1 = very reduce or absent. STF (ch 78, Prootic A).
83. Opisthotics, wide transverse occipital plane with depression for the nuchal musculature: 0 = absent; 1 = present. ST (ch 54); STF (ch 80, Opisthotic B).
84. Opisthotics, ventral ridge on opisthotic: 0 = absent; 1 = present, with an incipient enclosed middle ear region; 2 = present, but modified with an enclosed middle ear region. ST (ch 55); STF (ch 81, Opisthotic C).
85. Opisthotics, procesus interfenestralis: 0 = present, but not reaching the floor of cavum acustico-jugulare; 1 = present, reaching the floor of the cavum acustico-jugulare but small; 2 = present, reaching the floor of the cavum acustico-jugulare but robust. ST (ch 56); STF (ch 82, Opisthotic D). Ordered.
86. Basisphenoid, rostrum basisphenoidale: 0 = flat; 1 = rod-like, thick and rounded. JY2 (ch 56) & STF (ch 83) (Basisphenoid A); PH (ch 15); HY2, KL, & BR (ch 34).
87. Basisphenoid, paired pits on ventral surface of basisphenoid: 0 = absent; 1 = present. JY2 (ch 57) & STF (ch 84) (Basisphenoid B).
88. Basiphenoid, ventral surface: 0= flat to slightly convex, with posterior margin straight or slightly concave; 1= V-shaped crest, with posterior margin forming the basipterygoid process projected posterolaterally. Character combined from HY2, KL, & BR (ch 31 and 32), STF (ch 85, Basisphenoid C).
89. Basiphenoid, rough surface between basisphenoid and basioccipital: 0 = absent; 1 = present. STF (ch 87, Basisphenoid E).
90. Basiphenoid, dorsum sellae: 0 = low; 1 = high. PH (ch 16); HY2, Kl, & BR (ch 33). Remarks: coded for few fossils because: poorly described specimens, lack of figures detailing this feature, or obscured by rock matrix.
91. Basisphenoid, foramen caroticum laterale larger than foramen anterius canalis carotici interni: 0 = absent; 1 = present. PH (ch 5); HY2, KL, & BR (ch 37). Remarks: coded for few fossils because: poorly described specimens, lack of figures detailing this feature, or obscured by rock matrix.
92. Basiphenoid, foramen anterius canalis carotici interni visible in dorsalanterior view of basisphenoid: 0 = widely separated; 1 = close together. HY2, KL, & BR (ch 29). Remarks: coded for few fossils because: poorly described specimens, lack of figures detailing this feature, or obscured by rock matrix.
93. Hyomandibular, path of hyomandibular branch of the facial nerve: 0 = hyomandibular nerve passes through cranioquadrate space parallel to vena capitis lateralis; 1 = hyomandibular nerve runs independent from vena capitis lateralis. JY1 (ch 52) & STF (ch 95) (Hyomandibular Nerve A).
94. Stapedial Artery, size of foramen stapedio-temporale: 0 = relatively large (the size of a large blood foramina, ≥5 mm diameter); 1 = significantly reduced in size (the size of a nerve foramina, ≤3 mm diameter); 2 = absent. JY1 (ch 54) & STF (ch 90) (Stapedial Artery B). Remarks: we do not agree with the rationale of Anquetin (2012) and retain this as a multistate character. Ordered.
95. Stapedial Artery, foramen stapedio-temporale location in the otic chamber: 0 = on dorsal part and pointing dorsally; 1 = on the anterior wall of the otic region, pointing anteriorly. Reworded from STF (ch 91, Stapedial Artery C).
96. Recessus scalae tympani: 0 = almost nonexistent, not surrounded by bone; 1 = well developed. STF (ch 92, Recessus scalae tympani A).
97. Foramen jugulare posterius, relationship with the fenestra postotica: 0 = separate from fenestra postotica; 1 = coalescent with fenestra postotica. STF (ch 93, Foramen jugulare posterius A). Remarks: coded for few fossils because: poorly described specimens, lack of figures detailing this feature, or obscured by rock matrix.

98. Foramen nervi hypoglossi (XII), ventral covering: 0 = exposed in ventral view; 1 = covered in ventral view by an extension of the pterygoid and the basioccipital; 2 = covered in ventral view by an extension of the basioccipital. STF (ch 95, Foramen nervi hypoglossi A).
99. Internal Carotid Artery, splitting of the internal carotid artery and the cerebral and palatine arteries: 0 = not embedded in braincase bone elements, the cerebral artery enters at the foramen posterius canalis carotici cerebralis (known previously as the foramen caroticum basisphenoidale) in the basisphenoid; 1 = partially embedded, the internal carotid artery enters in the braincase elements through the foramen posterius canalis carotici interni, running along the pterygoid canal, and then splitting into the cerebral and palatine arteries at the fenestra caroticus; 2 = fully embedded, the internal carotid artery enters in the braincase elements through the foramen posterius canalis carotici interni, and split inside the braincase, lack of a ventral exposed fenestra caroticus. Combined character from HY2, KL, & BR (ch 30 and 36). Ordered.
100. Internal Carotid Artery, foramen posterius canalis carotici interny: 0 = absent; 1 = formed by pterygoid; 2 = formed by pterygoid and basisphenoid halfway along the basisphenoid-pterygoid suture; 3 = formed by prootic, prootic and basisphenoid, or prootic and pterygoid; 4 = formed by basisphenoid only. Reworded from JY1 (ch 56, Canalis Caroticum A); STF (ch 100, Canalis Caroticum G).
101. Palatine Artery, entering in the skull: 0 = through the interpterygoid vacuity or intrapterygoid slit; 1 = through the foramen posterius carotici palatinum between basisphenoid and pterygoid. Reworded from STF (ch 99, Canalis Caroticum F). Remarks: according to the definition of the foramina in Rabi et al. (2013), the entry of the palatine artery is through the foramen posterius carotici palatinum, known before as the foramen caroticum laterale.
102. Fenestra Perilymphatica: 0 = large; 1 = reduced in size to that of a small foramen. JY1 (ch 57) & STF (ch 101) (Fenestra Perilymphatica A). Remarks: coded for few fossils because: poorly described specimens, lack of figures detailing this feature, or obscured by rock matrix.
103. Cranial scutes, scute D meeting in midline: 0 = absent; 1 = present. STF (ch 103) (Cranial Scute B).
104. Cranial scutes, scute X much smaller than scute D: 0 = absent; 1 = present. STF (ch 104) (Cranial Scute C).
105. Cranial scutes, scute X partially separates scutes G: 0 = absent; 1 = present. STF (ch 105) (Cranial Scute D).
106. Cranial scutes, scutes A, B, and C forming a continus posterolateral shelf: 0 = absent; 1 = present. STF (ch 106) (Cranial Scute E).
107. Cranial scutes, scute F: 0 = formed by several scutes; 1 = formed by a single scute. STF (ch 116) (Cranial Scute O).
108. Cranial scutes, scute J: 0 = formed by several scutes; 1 = formed by a single scute. STF (ch 117) (Cranial Scute P).

Lower Jaw

109. Dentary, medial contact of dentaries: 0 = fused; 1 = open suture. JY1 (ch 58) & STF (ch 120) (Dentary A).
110. Dentary, width triturating surface vs jaw length: 0 = narrow triturating surface, symphysis less than 1/3 of jaw length; 1 = broad triturating surface, symphysis ≥1/3 jaw length. Reworded from HY2, KL, & BR (ch 39).
111. Dentary, symphyseal ridge: 0 = absent, flat triturating surface; 1 = present, but not visible in lateral view, flat to slightly convex triturating surface; 2 = present and greatly developed, visible in lateral view, ridge along entire length of symphysis. Reworded from HY2 (ch 41 & 42); PH (ch 6), & KL (ch 41). Ordered.
112. Dentary, lingual (tomial) ridge: 0 = prominent; 1 = weak or absent. HY2 (ch 43), PH (ch 7), KL & BR (ch 42).
113. Dentary-Surangular arrangement: 0 = lack of a posterior expansion of dentary and anterior projection of surangular; 1 = posterior expansion of dentary present almost reaching the articular surface, covering the dorsal half of the surangular in lateral view, surangular with anterior projection. HY2 (ch 44), PH (ch 8). Reworded from KL (ch 43).
114. Splenial: 0 = present; 1 = absent. JY1 (ch 59, Splenial A); HY2 (ch 45); KL & BR (ch 44).

Carapace

115. Carapace, carapacial scutes: 0 = present; 1 = reduced not fully covering the carapace; 2 = absent. Reworded from JY1 (ch 60) & STF (ch 121) (Carapace A) and HY2, KL & BR (ch 80). Joyce's (2007) original wording for the character is somewhat confusing, as it is unclear how carapacial scutes might be "partially present." The original intention of this character was to capture the presence of carapacial scutes in some turtles that only cover part of the shell. This condition is found in *Mesodermochelys undulatus* and *Pseudanosteira pulchra*. Scutes are also found in juvenile individuals of *Carettochelys insculpta* (Zangerl 1959). We do not follow the reduction of this character to two character states, as proposed by Anquetin (2012). Ordered.
116. Carapace, three parallel lines of keels: 0 = absent; 1 = present, but only poorly developed; 2 = present and

pronounced; 3 = present, but only with a medial line of keels on neurals, absence of keels on costals. JY1 (ch 61) & STF (ch 122) (Carapace B) and HY2, KL, & BR (ch 84). We do not follow the proposed reduction of this character to two character states (Anquetin 2012, character 88). Remarks: Sterli and de la Fuente (2013) coded *Araripemys barretoi* as (2), but examination of the holotype indicates that is poorly developed, changed here to (1). Also *Platychelys oberndorferi* is changed here from (0) to (1). A third state was added to include forms with a single medial line of keels as in protostegids and some cheloniids.

117. Shell, sculpturing of dorsal surface (carapace) and ventral surface (plastron): 0 = absent, smooth to slightly rugose; 1 = present, development of striations, vermiculations, striations, or pitting. Modified from STF (ch 124) (Carapace D). Remarks: *Proganochelys quenstedti* is coded here as (0&1) with marked striations in the posterior portion of the carapace.
118. Shell, pattern of sculpturing of the dorsal surface (carapace) and ventral surface (plastron): 0 = parallel to radial striations; 1 = vermiculation; 2 = highly dense pattern of pitting combined with striations; 3 = dichotomic striations; 4 = spread pitting without marked striation pattern; 5 = granules (positive relief). Modified from STF (ch 125) (Carapace E).
119. Carapacial Sutures: 0 = carapacial elements finely sutured or the contact is smooth; 1 = carapacial sutures strongly serrated in adult stage. Character from Zhou et al. (2014) (ch 244).
120. Nuchal, articulation of nuchal with neural spine of eighth cervical vertebra: 0 = cervical articulates with nuchal along a blunt facet; 1 = articulation absent; 2 = cervical articulates with nuchal along a raised pedestal. JY1 (ch 62) & STF (ch 126) (Nuchal A). We do not follow Anquetin (2012) and retain this character as a single multistate character.
121. Nuchal, elongate costiform process: 0 = absent; 1 = present, crosses peripheral 1; 2 = present, well developed reaches peripherals 2 or 3. Modified from JY1 (ch 63) & STF (ch 127) (Nuchal B). Remarks: we adjust the scoring of *Baptemys wyomingensis* and *Dermatemys mawii* to 1 (Knauss et al. 2011). State (1) was splitted in state (1) and (2). Ordered.
122. Nuchal, length versus width: 0 = wider than long; 1 = longer than wide or as long as wide. de la Fuente (2003) & STF (ch 128) (Nuchal C).
123. Nuchal, posteriomedial fontanelles: 0 = absent; 1 = present. HY2, KL, & BR (ch 81) & PH (ch 30). Remarks: Bardet et al. (2013) coded as present for *Erquelinnesia gosseleti* (Zangerl 1971).
124. Neurals, neural formula 6>4<6<6<6<6: 0 = absent; 1 = present. JY1 (ch 64) & STF (ch 129) (Neural A).
125. Neurals, shape of neurals: 0 = very irregular in shape, wider than long or squared; 1 = regular, often perfectly hexagonal or pentagonal, longer than wide. STF (ch 130) (Neural B) & HY2, KL & BR (ch 86).
126. Neurals, number of neurals: 0 = ten or more; 1 = nine or less; 3 = COall neurals lost even in ventral view. Modified character from HY2, KL & BR (ch 85 & ch 87) and PH (ch 33). State character (3) reworded. Remarks: a combined character from HY2 (ch 85 & ch 87) is proposed here that covers all the possible variations in the number and reduction of neurals.
127. Peripheral Gutter: 0 = peripheral gutter absent of only anteriorly developed; 1 = peripheral gutter extensively developed along anterior and bridge peripherals. Character from Zhou et al. (2014) (ch 246).
128. Peripherals, number of peripherals: 0 = more than 11 pairs of peripherals present; 1 = 11 pairs of peripherals present; 2 = 10 pairs of peripherals present; 3 = less than 10 pairs of peripherals present. JY1 (ch 65) & STF (ch 131) (Peripheral A). Remarks: we do not follow Anquetin (2012) and retain this character as a single multistate character. Ordered.
129. Peripherals, anterior peripherals incised by musk ducts: 0 = absent; 1 = present. JY1 (ch 66) & STF (132) (Peripheral B).
130. Costals, medial contact of the first pair of costals: 0 = absent; 1 = present. Reworded from JY1 (ch 67) & STF (ch 133) (Costal A).
131. Costals, medial contact of posterior costals: 0 = absent; 1 = medial contact of up to three posterior costals present; 2 = medial contact of all costals present. Modified from JY1 (ch 68) & STF (ch 134) (Costal B). Remarks: we do not follow Anquetin (2012) and retain this character as a single multistate character. However, we follow Anquetin (2012) by adjusting the scoring for *Mesodermochelys undulatus*. Ordered.
132. Costals, distal rib end and lateral ossification of the costal: 0 = costals fully ossified laterally with strong sutural contact with peripherals, lack of dorsal exposure of distal end of costal ribs; 1 = costals fully ossified laterally with strong sutural contact with peripherals, distal end of costal ribs exposed on dorsal surface and surrounded by the peripheral; 2 = costals lack lateral ossification, allowing the dorsal exposure of the distal end of ribs and the development of fontanelles only at the most anterior and posterior costals; 3 = costals with extreme lost of lateral ossification, allowing the dorsal exposure of the distal end of ribs, in almost all series of costals. Remarks: character reworded from STF (ch

135) (Costal C) and the combination of characters (ch 243) (costal rib) and (ch 247) (costal rib distal end) from Zhou et al. (2014).

133. Rib free peripherals: 0 = absent; 1 = present, only anterior and posterior to ribs; 2 = present, between sixth and seventh ribs; 3 = present, between seventh and eighth ribs. Reworded from PH (ch 29).
134. Costals, alternative short and long ends in the lateral part of costals: 0 = absent; 1 = present. STF (ch 136) (Costal D).
135. Costals, costal 9: 0 = present; 1 = absent. Reworded from HY2, KL & BR (ch 90).
136. Costals, shape of Costal 3: 0 = tapering towards the lateral side of the shell or with parallel anterior and posterior borders; 1 = broadens towards the lateral side of the shell. Character from Zhou et al. (2014) (ch 242).
137. Suprapygals, number of suprapygals: 0 = one; 1 = two; 2 = more than two; 3 = absent. Hirayama et al. (2000) and STF (ch 137) (Suprapygal A). Ordered.
138. Suprapygals, size between suprapygal 1 and 2: 0 = suprapygal 1 smaller than suprapygal 2; 1 = suprapygal 1 larger. Reworded from KL (ch 88). Remarks: turtles with only one suprapygal or suprapygals absent are coding as (-).
139. Cervical scute: 0 = more than one cervical scute present; 1 = one cervical scute present; 2 = cervical scutes absent, carapacial scutes otherwise present. JY1 (ch 70) & STF (ch 138) (Cervical A). Remarks: we do not follow Anquetin (2012) and retain the original multistate arrangement for this character.
140. Pygal, posterior notch: 0 = present; 1 = absent. Modified from Lapparent de Broin and Murelaga (1999) & PH (ch 35).
141. Supramarginals: 0 = complete row present, fully separating marginals from pleurals; 1 = partial row present, incompletely separating marginals from pleurals; 2 = absent. JY1 (ch 71) & STF (ch 139) (Supramarginal A). Remarks: we do not follow Anquetin (2012) and retain the original multistate arrangement for this character. We furthermore retain the scoring of *Platychelys oberndorferi* as 1, as this taxon clearly exhibits supramarginals (Bräm 1965). The Munich specimens are not informative in this regard, as the lateral portions of the shell are not preserved. In addition to its supramarginals, *P. oberndorferi* also possesses supernumerary pleural scales (Joyce 2003). Ordered.
142. Vertebrals, shape of the verterbrals: 0 = vertebrals 2 to 4 significantly broader than pleurals; 1 = vertebrals 2 to 4 as narrow as, or narrower than, pleurals. JY1 (ch 73) & STF (ch 141) (Verterbal B).
143. Vertebrals, position of vertebral 3-4 sulcus in taxa with five vertebrals: 0 = sulcus positioned on neural 6; 1 = sulcus positioned on neural 5. JY1 (ch 74) & STF (142) (Vertebral C).
144. Vertebrals, vertebral 3-4 sulcus with a wide posteriorly oriented medial embayment: 0 = absent; 1 = present. AN (ch 108).
145. Vertebrals, verebral 1: 0 = vertebral 1 does not enter anterior margin of carapace; 1 = enters anterior margin. Character from Zhou et al. (2014) (ch 245).
146. Marginals, marginal scutes overlap onto costals: 0 = absent, marginals restricted to peripherals; 1 = present. Meylan and Gaffney (1989) & STF (ch 143) (Marginal A).
147. Pleurals, at least one pair of additional pleural scutes located laterally of vertebral scute 1, with anterior contact with cervical scute: 0 = absent; 1 = present. Modified from PH (ch 32).

Plastron

148. Plastron, connection between carapace and plastron: 0 = osseous; 1 = ligamentous. JY1 (ch 75) & STF (ch 144) (Plastron A). Remarks: we adjust Anquetin (2012) scoring of *Odontochelys semitestacea* to 1, as it is apparent that a turtle lacking peripherals can only have a ligamentous bridge.
149. Plastron, central plastral fontanelle: 0 = absent; 1 = present. Modified from JY1 (ch 76) & STF (ch 145) (Plastron B) and HY2, KL & BR (ch 97). Remarks: see recommendation in Character 143 about levels of ossification and ontogeny.
150. Plastron, posterior plastral fontanelle, posterior plastral fontanelle between the xiphiplastra and/or the hypoplastra: 0 = absent in adult stage; 1 = retained in adult stage. Character from Zhou et al. (2014) (ch 239).
151. Plastron, plastral kinesis: 0 = absent, scutes sulci and bony sutures do not overlap; 1 = present, scutes sulci coincide with epiplastral-hyoplastral contact. JY1 (ch 77, Plastron C).
152. Plastron, plastral kinesis: 0 = between hyoplastron and hypoplastron; 1 = between hyoplastron and epiplastron-entoplastron. STF (ch 148) (Plastral Kinesis B).
153. Plastron, hyo-hypoplastra contact and shape: 0 = deep U or V-shaped axillar and inguinal notches, contact between hyo-hyoplastra absent or reduced due to the presence of mesoplastra or a central fotanelle; 1 = deep axillar and inguinal notches, reduced contact between both elements due to the existence of central and lateral fontanelles; 2 = deep axillar and inguinal notches, extensive contact between hyo-hyoplastra (even for

those taxa with plastral kinesis); 3 = a very narrow to absent contact between each other, star-shaped with extremely serrate medial edges, very shallow axillar and inguinal notches, and long lateral edges; 4 = extreme loss of ossification of hyo-hypoplastra, lack of contact between each other. Combined from HY2, KL & BR (ch 96) and PH (ch 28). Remarks: two states were added to cover all possible variations in the contact between hyo-hypoplastra and the shape of both elements related to the presence of mesoplastra or fontanelles.

154. Entoplastron: 0 = present; 1 = absent. STF (ch 153) (Entoplastron E).
155. Entoplastron, anterior entoplastral process: 0 = present, medial contact of epiplastra absent; 1 = absent, medial contact of epiplastra present. JY1 (ch 78) & STF (ch 149) (Entoplastron A).
156. Entoplastron, size of the posterior entoplastral process: 0 = posterior process long, reaching as far posteriorly as the mesoplastra; 1 = posterior process reduced in length. JY1 (ch 79) & STF (150) (Entoplastron B).
157. Entoplastron, distinct posterolateral process: 0 = present; 1 = absent. JY1 (ch 80) & STF (ch 151) (Entoplastron C).
158. Entoplastron, shape of the entoplastron in ventral view: 0 = dagger-shaped; 1 = massive diamond-shaped; 2 = T-shaped, longer than wide; 3 = T-shaped, wider than long, forming broad lateral wings; 4 = strap like and V-shaped. Combined from JY1 (ch 81) & STF (ch 152) (Entoplastron D); AN (ch 116); and HY2, KL & BR (ch 101).
159. Entoplastron, suture with hyoplastra: 0 = tightly sutured; 1 = lightly sutured to almost absent contact between both. Modified from HY2, KL & BR (ch 99), and STF (ch 154) (Entoplastron F).
160. Epiplastra, shape and contact of epiplastra: 0 = epiplastra squarish in shape, lack a contact between each other due to the narrow participation of the entoplastron in the anterior plastral lobe edge; 1 = epiplastra elongate in shape, with medial contact located anterior to the entoplastron; 2 = epiplastra squarish in shape lack of medial contact due to the extensive anterior and lateral projections of the entoplastron. Modified from JY1 (ch 83, Epiplastron A). Remarks: A third state is added to describe variations in the participation of the entoplastron to the anterior plastral lobe edge.
161. Epiplastra, very thick anterior lip in dorsal view: 0 = present; 1 = absent. Hirayama et al. (2000) and STF (ch 156) (Epiplastron B).
162. Hyoplastra, contacts of axillary buttresses: 0 = absent to slightly contacting peripherals only; 1 = peripherals and costal 1. Modified from JY1 (ch 84) & STF (ch 157) (Hyoplastron A) and HY2, KL & BR (ch 92).
163. Hyoplastra, termination of axillary buttresses: 0 = terminates on peripheral 1 or 2; 1 = terminates on peripheral 3; 2 = terminates on peripheral 4 or 5 level; 3 = ossified axillary buttresses absent. Reworded from Hutchison (1991) and STF (ch 159) (Hyoplastron B).
164. Mesoplastron: 0 = two present; 1 = one present; 2 = absent. Modified from JY1 (ch 85) & STF (ch 160) (Mesoplastron A) and AN (ch 120 and ch 121). Remarks: we follow Sterli (2008) and Anquetin (2012) by splitting character 85 of Joyce (2007), but instead of three new characters, we only create two, one of which is multistate. Ordered.
165. Mesoplastron, medial contact of mesoplastra: 0 = present, or virtually present when a central plastral fontanelle is present, absence of contact between hyoplastron and hypoplastron; 1 = absent, partial contact between hyoplastron and hypoplastron present. Modified from JY1 (ch 85) & STF (ch 160) (Mesoplastron A) and AN (ch 122). Remarks: we use the reworded character of Anquetin (2012) and follow his scoring for this character as well.
166. Hypoplastra, contacts of inguinal buttresses: 0 = absent to slightly contacting peripherals; 1 = peripheral and costal 5; 2 = peripheral, costals 5 and 6; 3 = peripherals and costal 4. Modified from JY1 (ch 86) & STF (ch 161) (Hypoplastron A); AN (ch 123) and HY2, KL & BR (ch 93). Remarks: a third state is added for the condition in *Chelus fimbriata*, having an inguinal buttress restricted to costal 4 and peripherals.
167. Hypoplastra, termination of inguinal buttresses: 0 = peripheral 8; 1 = peripheral 7; 2 = peripheral 6. Iverson (1991) and STF (ch 162) (Hypoplastron B). Ordered.
168. Xiphiplastra, distinct anal notch: 0 = absent; 1 = present. JY1 (ch 87) & STF (163) (Xiphiplastron A).
169. Xiphiplastra, shape of xiphiplastra: 0 = almost triangular to trapezoidal, with lateral straight to convex margin; 1 = rectangular elongated in shape, coupled forming together with the hypoplastron a very narrow posterior plastral lobe; 2 = narrow struts, separated by the posterior fontanelle. Reworded from JY1 (ch 88) & STF (ch 164) (Xiphiplastron B) and HY2, KL & BR (chs 102, 103 and 104). Remarks: Zhou et al. (2014) proposed a new character (Plastron lobe, ch 241) for the posterior plastral lobe, however this becomes a redundant character because the shape of the posterior plastral lobe is mostly determinate by the shape of the xiphiplastron, and we combine this character with the previously defined character 88 of Joyce (2007). However, we split the character state 1 in two: covering the

two most common shapes of the xiphiplastron related to the shape of the posterior plastral lobe.

170. Plastral scutes: 0 = present; 1 = absent. JY1 (ch 89) & STF (ch 165) (Plastral scutes A) and HY2, KL & BR (ch 57).
171. Plastral scutes, midline sulcus: 0 = straight; 1 = distinctly sinuous, at least for part of its length. AN (ch 127) & STF (ch 166) (Plastral scutes B).
172. Gular, number of gulars: 0 = one pair of scutes; 1 = only one scute. Reworded from JY1 (ch 91) & STF (ch 167) (Gular A).
173. Extragulars: 0 = present; 1 = absent. JY1 (ch 92) & STF (ch 168) (Extragular A).
174. Extagulars, medial contact: 0 = absent; 1 = present, contacting one another anterior to gular(s); 2 = present, contacting one another posterior to gular(s). JY1 (ch 93) & STF (ch 169) (Extragular B). Remarks: Even though character state 2 is only developed in *Chelodina oblonga*, we retain this character as a multistate character, contra to Anquetin (2012).
175. Extragulars, anterior plastral tuberosities: 0 = present; 1 = absent. JY1 (ch 94) & STF (ch 170) (Extragular C). Remarks: we disagree in the coding for *Chelus frimbriata* and *Otwayemys cunicularius*, both taxa lack of strong tuberosities as the one in stem-testudines, coding as (1) for both here.
176. Extragulars, restricted to epiplastra: 0 = present; 1 = absent, extragulars reach the entoplastron. Reworded from An (ch 129) & STF (ch 171) (Extragular D).
177. Intergulars: 0 = absent; 1 = present. JY1 (ch 95) & STF (ch 172) (Intergular A).
178. Humerals, number of pairs: 0 = one pair present; 1 = two pairs present, subdivided by a plastral hinge. JY1 (ch 96) & STF (ch 173) (Humeral A).
179. Humerals, humero-pectoral sulcus: 0 = restricted to hyoplastra; 1 = crossing the posterior portion of entoplastron. STF (ch 174) (Humeral B). Remarks: in extant cheloniids, this character is polymorphic, depending of the length of the posterior process of the entoplastron. This could be also the condition for most marine forms for which this character can be coded due to poor illustrations or bad preservation of sulci.
180. Pectorals: 0 = present; 1 = absent. JY1 (ch 97) & STF (ch 175) (Pectoral A).
181. Pectorals, antero-posteriorly developed: 0 = present; 1 = absent, very short antero-posterior development. STF (ch 176) (Pectoral B).
182. Abdominals: 0 = present, in medial contact with one another; 1 = present, medial contact absent; 2 = absent. JY1 (ch 98) & STF (ch 177) (Abdominal A). Remarks: we do not follow Anquetin (2012) and retain the original multistate nature of this character. The scoring of *Emarginachelys cretacea* is amended to 1 (pers. comn. of WGJ of type material). Ordered.
183. Anals: 0 = only cover parts of the xiphiplastra; 1 = overlap anteromedially onto the hypoplastra. JY1 (ch 99) & STF (ch 178) (Anal A) and HY2, KL & BR (ch 94)
184. Inframarginals: 0 = more than two pair present, plastral scales do not contact marginals; 1 = two pair present (axillaries and inguinals), limited contact between plastral scales and marginals present; 2 = absent, unrestricted contact between plastral scales and marginals present. JY1 (ch 100, Inframarginal A) & STF (ch 179, 180, and 181) (Inframarginals, A, B and C). Remarks: we do not follow Anquetin (2012) or Sterli and de la Fuente (2013) and retain the original multistate nature of this character. We furthermore adjust the scoring of all kinosternids from 0 to 1 (Knauss et al. 2011). Ordered.

Neck

185. Cervical ribs: 0 = large cervical ribs present; 1 = cervical ribs reduced or absent. JY1 (ch 101) & STF (ch 182) (Cervical Rib A). Remarks: we follow Anquetin (2012) correction for the scoring of *Palaeochersis talampayensis*.
186. Cervicals, position of the transverse processes: 0 = middle of the centrum; 1 = anterior end of the centrum. JY1 (ch 102) & STF (ch 183) (Cervical Vertebra A).
187. Cervicals, posterior cervicals with strongly developed ventral keels: 0 = absent or slightly developed in all vertebrae; 1 = present, more developed on posterior vertebrae. JY1 (ch 103) & STF (ch 184) (Cervical Vertebra B); HY2 (ch 48); and KL & Br (ch 47).
188. Cervicals, cervical 8 centrum significantly shorter than cervical 7: 0 = absent; 1 = present. JY1 (ch 104) & STF (ch 185) (Cervical Vertebra C) and HY2, KL & BR (ch 52).
189. Cervicals, triangular diapophyses: 0 = absent; 1 = present. Gaffney (1996) and STF (ch 186) (Cervical Vertebra D).
190. Cervicals, central articulations of cervical vertebrae: 0 = articulations not formed, cervical vertebrae amphicoelous or platycoelous; 1 = articulations formed, cervical vertebrae procoelous or opisthocoelous. JY1 (ch 105) & STF (ch 187) (Cervical Articulation A); HY2 (ch 49); and Kl & BR (ch 48). Remarks: Bardet et al. (2013) coded *Notochelone* as amphicoelous based on the descriptions from Gaffney (1981).

191. Cervicals, articulation between cervical 8 and dorsal vertebrae 1: 0 = 8(dorsal 1; 1 = 8)dorsal 1; 2 = none, vertebrae only meet at zygapophyses. JY1 (ch 112) & STF (ch 188) (Cervical Articulation H) and RH2, KL & BR (ch 51). Remarks: we do not follow Anquetin (2012) and retain the original multistate character of Joyce (2007).
192. Cervicals, biconvex cervical vertebrae in the middle of the neck: 0 = absent; 1 = present. STF (ch 189) (Cervical Vertebra E).
193. Cervicals, biconvex cervical vertebra in the middle of the neck: 0 = cervical 2; 1 = cervical 3; 2 = cervical 4; 3 = cervical 5. JY1 (ch 106) (Cervical Articulation B, C & D); STF (ch 190) (Cervical Vertebra F).
194. Cervicals, biconcave cervical vertebrae: 0 = absent; 1 = present. STF (ch 191) (Cervical Vertebra G).
195. Cervicals, double articulation between cervical 5 and 6: 0 = absent; 1 = present. JY1 (ch 109) (Cervical Articulation E); STF (ch 192) (Cervical Vertebra I).
196. Cervicals, double articulation between cervical 6 and 7: 0 = absent; 1 = present. JY1 (ch 110) (Cervical Articulation F); STF (ch 193) (Cervical Vertebra J).
197. Cervicals, central articulation between cervical 6 and 7: 0 = cervical 6 concave (cervical 7 convex; 1 = platycoelous, cervical 6 II cervical 7. JY1 (ch 110) (Cervical Articulation F); STF (ch 194) (Cervical Vertebra K).
198. Cervicals, double articulation between cervical 7 and 8: 0 = absent; 1 = present. JY1 (ch 111) (Cervical Articulation G); STF (ch 195) (Cervical Vertebra L); PH (ch 27); and RH2, KL & BR (ch 51 and 53).
199. Cervicals, height versus length of centra and neural arch: 0 = total height of centra and neural arch longer than the anteroposterior length of the cervical centra; 1 = total height of centra and neural arch much shorter than the anteroposterior length of the cervical centra. STF (ch 196) (Cervical Vertebra H).
200. Cervicals, modification of neural arch on cervical 8: 0 = neural arch without modificiation of postzygapophyses; 1 = neural arch with postzygapophyses poiting anteroventrally. STF (ch 197) (Cervical Vertebra I).
201. Cervicals, postzygapophyses united in midline: 0 = absent; 1 = present. Bona and de la Fuente (2005); STF (ch 198) (Cervical Vertebra J).
202. Cervicals, ventral process on cervical 8: 0 = absent; 1 = present, well developed (as tall or taller than the height of the centrum). STF (ch 199) (Cervical Vertebra K).
203. Cervicals, shape of central articulation of cervicals 7 and 8: 0 = as high as wide; 1 = much wider than high. Reworded from HY2 (ch 47), KL & BR (ch 46).

Ribs

204. Ribs, length of first dorsal rib: 0 = long, extends full length of first costal and may even contact peripherals distally; 1 = intermediate, in contact with well-developed anterior bridge buttresses; 2 = intermediate to short, extends less than halfway across first costal. JY1 (ch 113) & STF (ch 200) (Dorsal Rib A) and HY2, KL & BR (ch 55). Remarks: although we agree with Anquetin (2012) that the anterior plastral buttress cannot be used as a fixed reference when assessing the length of the first thoracic, our experience with this character demonstrates that all turtle clearly fall into the three classes developed as character states herein. We therefore maintain the character of Joyce (2007) as originally developed. Ordered.
205. Ribs, contact of dorsal ribs 9 and 10 with costals: 0 = present; 1 = absent. JY1 (ch 114) & STF (ch 201) (Dorsal Rib B).
206. Dorsal rib 10: 0 = long, spanning full length of costals and contacting peripherals distally; 1 = short, not spanning father distally than pelvis. JY1 (ch 115) & STF (ch 202) (Dorsal Rib C), HY2, KL & BR (ch 56). Remarks: we follow Anquetin's (2012) adjustment in the scoring of *Santachelys gaffneyi*.

Vertebrae

207. Dorsals, anterior articulation of the first dorsal centrum: 0 = faces at most slightly anteroventrally; 1 = faces strongly anteroventrally. JY1 (ch 116) & STF (ch 203) (Dorsal Vertebra A) and HY2, KL & BR (ch 54)

Tail

208. Caudals, tail club: 0 = present; 1 = absent. JY1 (ch 118) & STF (ch 204) (Caudal A).
209. Caudals, caudal centra: 0 = all centra amphicoelous; 1 = all centra more or less pronounced procoelous; 2 = all centra more or less pronounced opisthocoelous; 3 = anterior few centra procoelous, posterior centra predominantly opisthocoelous. JY1 (ch 119) & STF (ch 205) (Caudal B) and HY2, KL & BR (ch 58 and 59). Remarks: we do not follow Anquetin (2012) and retain the original multistate character of Joyce (2007).
210. Caudals, anterior caudal centra: 0 = amphicoelous; 1 = procoelous or platycoelous; 2 = opisthocoelous. STF (ch 206) (Caudal C).
211. Caudals, posterior caudal centra: 0 = amphicoelous; 1 = procoelous or platycoelous: 2 = opisthocoelous. STF (ch 207) (Caudal D).

212. Caudals, chevrons: 0 = present on nearly all caudal vertebrae; 1 = absent, or only poorly developed, along the posterior caudal vertebrae. JY1 (ch 117) & STF (ch 207) (Chevron A) and HY2, KL & BR (ch 57).
213. Caudals, tail ring: 0 = absent; 1 = present. STF (ch 208) (Tail Ring A).

Pectoral girdle

214. Scapula, anterodorsal ridge of acromion: 0 = present; 1 = absent. New character. Remarks: the acromion ridge of basal turtles such as *Proganochelys quenstedti* is triradiate in cross section due to the developed of three ridges. The anterodorsal ridge (sensu Gaffney 1990) runs from the acromion to the dorsal process of the scapula. The ventral ridge (sensu Gaffney 1990; acromion ridge sensu Joyce 2007) runs from the acromion to the glenoid. The horizontal ridge (sensu Gaffney 1990) spans between the acromion and the coracoid and may contain the coracoid foramen. These three ridges are apparent lost in steps independently from one another and we therefore reorganize characters 122 and 124 of Joyce (2007) into three characters, one of which of multistate. These character partially contain the morphologies discussed by Sterli (2007, character 75) and Anquetin (2012, character 165).
215. Scapula, ventral ridge of acromion: 0 = present; 1 = absent developed proximally near glenoid. Reworded from JY1 (ch 122, Scapula B).
216. Scapula, horizontal ridge of acromion: 0 = well-developed, coracoid foramen present; 1 = reduced, only developed along distal portion of acromion. Modified from JY1 (ch 124, Coracoid A). Ordered.
217. Scapula, glenoid neck on scapula: 0 = absent; 1 = present. JY1 (ch 123, Scapula C).
218. Scapula, lamina between the dorsal process of the scapula and the acromion: 0 = well developed; 1 = reduced; 2 = absent. STF (ch 215) (Scapula A). Ordered.
219. Scapula, internal angle between acromion process and scapular process ≥110º: 0 = absent; 1 = present. Reworded from PH (ch 18) and HY2, KL & BR (ch 61).
220. Coracoid, coracoid vs humerus length: 0 = shorter than humerus; 1 = at least as long as humerus. PH (ch 26) and HY2, KL & BR (ch 60).
221. Coracoid, foramen: 0 = present; 1 = absent. Gaffney et al. (2007) and Joyce et al. (2013) (ch 82).
222. Cleithrum: 0 = present and in contact with the carapace; 1 = present, osseous contact with carapace absent; 2 = absent. JY1 (ch 120) & STF (ch 214) (Cleithrum A). Ordered.

Pelvic girdle

223. Pelvis, pelvis-shell attachment: 0 = pelvis-shell attachment by ligaments; 1 = pelvis attached by strong sutural contact of the ischium and pubis with the plastron, and illium with the carapace. ST (ch 138); JY1 (ch 134) & STF (ch 221) (Pelvis A). Remarks: States 1 and 2 of STF combined in one, considering that one of them is only apomorphic for Palaeochersis
224. Pelvis, thyroid fenestra: 0 = coalescent; 1 = two separated fenestra completely or partially separated. STF (ch 222) (Pelvis B).
225. Ilium, elongated iliac neck: 0 = absent; 1 = present. JY1 (ch 126) & STF (ch 225) (Ilium A).
226. Ilium, iliac scar: 0 = extends from costals onto the peripherals and pygal; 1 = positioned on costals only. JY1 (ch 127) & STF (ch 226) (Ilium B).
227. Ilium, shape of the ilium articular site on the visceral surface of the carapace: 0 = narrow and pointed posteriorly; 1 = oval. JY1 (ch 128) & STF (ch 227) (Ilium C).
228. Ilium, posterior notch in acetabulum: 0 = absent; 1 = present. JY1 (ch 129) & STF (ch 228) (Ilium D).
229. Ilium, thelial process: 0 = absent; 1 = present. Meylan (1987); STF (ch 229) (Ilium E).
230. Pubis, lateral process: 0 = small, poorly developed, columnar; 1 = well developed and flat. STF (ch 223) (Pubis A); HY2, KL & BR (ch 62).
231. Pubis, epipubis process: 0 = osseus or calcified; 1 = cartilaginous or absent. STF (ch 224) (Pubis B).
232. Ischium, ischial contacts with plastron: 0 = contact via a large central tubercle; 1 = contact via two separate ischial processes. JY1 (ch 130, Ischium A).
233. Ischium, lateral process of ischium or metischial process: 0 = absent; 1 = present. PH (ch 19); HY2, KL & BR (ch 64); STF (ch 230) (Ischium A).
234. Hypoischium: 0 = present; 1 = absent. JY1 (ch 131, Hypoischium A).

Forelimb

235. Humerus, ectepicondylar foramen: 0 = in a channel; 1 = only a groove. Meylan (1987) & STF (ch 216) (Humerus A).
236. Humerus, proximal articular surface of humerus: 0 = with shoulder on preaxial side, upturned; 1 = without shoulder, not upturned. Gaffney (1990); HY2, KL & BR (ch 68); STF (ch 217) (Humerus B).
237. Humerus, lateral process of humerus: 0 = abuts caput humeri; 1 = slightly separated from caput humeri; 2 = located distal to caput humeri but along proximal end

of shaft; 3 = located at middle of humeral shaft. HY2, KL & BR (ch 67); STF (ch 218) (Humerus C). Ordered.

238. Humerus, lateral process of humerus: 0 = visible in dorsal view: 1 = not visible in dorsal view. STF (ch 219) (Humerus D).
239. Humerus, lateral process shape: 0 = rounded to slightly squared; 1 = V-shaped or triangular. Reworded from PH (ch 25) and HY2, KL & BR (ch 70).
240. Humerus, expansion of lateral process: 0 = limited to anterior surface of shaft; 1 = expands onto ventral surface. Reworded from HY2, KL & BR (ch 71).
241. Humerus, medial concavity of lateral process: 0 = absent; 1 = present. HY2, KL & BR (ch 72).
242. Humerus, prominent anterior projection of lateral process: 0 = absent; 1 = present. HY2, KL & BR (ch 73).
243. Humerus, length of the humerus versus the width of the proximal end: 0 = two times or less the width of the proximal end: 1 = more than two times the width of the proximal end. STF (ch 220) (Humerus E).
244. Humerus, scar for Muscle latissimus dorsi and Muscle teres major: 0 = located anterior to humeral shaft; 1 = located at middle of shaft. HY2, KL & BR (ch 69).
245. Humerus, humerus length vs femur length: 0 = shorter than femur; 1 = longer than femur. HY2, KL & BR (ch 66).
246. Ulna, contact with radius through rugosity and ridge: 0 = absent; 1 = present. HY2, KL & BR (ch 74).
247. Radius, curves towards anterior: 0 = absent; 1 = present. HY2, KL & BR (ch 75).
248. Manus, phalangeal formula of the manus: 0 = most digits with two shortenened phalanges: 1 = most digits with three elongated phalanges. JY1 (ch 132) & STF (ch 232) (Manus A).
249. Manus, paddles: 0 = absent, moveable articulations of all digits; 1 = 'half-paddle' digits 3 and 5 modified into paddle with rigid articulations. But digits 1 and 2 immoveable; 2 = elongate paddles present, digits 1 and 2 modified into paddle with rigid articulations, and very flat carpal and tarsal elements. Combined from JY1 (ch 133, Manus B) and HY2, KL & BR (chs 76, 77 and 78). Remarks: we do not follow Anquetin (2012) and retain this as a multistate character. Ordered.
250. Manus, flippers: 0 = absent; 1 = short flippers present; 2 = elongate flippers present. JY1 (ch 134, Manus C). Remarks: we do not share Anquetin (2012) reservation in regards to this character and leave it in the matrix. Ordered.
251. Ulnare, size of the ulnare vs the intermedium: 0 = smaller than intermedium: 1 = nearly as large as intermedium; 2 = much larger than intermedium. Remarks: character defined by Tong et al. (2006), but first time included in a phylogenetic analysis. New character. Ordered.

Hindlimb

252. Pes, number of digits: 0 = five; 1 = four. STF (ch 237) (Pes C).
253. Manus and Pes, flattening of carpals and tarsal elements: 0 = absent; 1 = present. HY2, KL & BR (ch 76); STF (ch 238) (Manus and Pes A).
254. Manus and Pes, hyperphalangy manus digits 4 and 5, pes digit 4: 0 = absent; 1 = present. Meylan (1987) & STF (ch 239) (Manus and Pes B).
255. Femur, femoral trochanters: 0 = distinct, and separated from one another; 1 = fossa obliterated, space between trochanters not concave, but notch present; 2 = fossa obliterated, trochanters connected by bony ridge without a notch. Character combined from HY2, KL & BR (ch 79) and PH (ch 20 and ch 21). Ordered.
256. Tibia, tibial pit for pubotibialis and flexor tibialis internus muscles: 0 = absent; 1 = present. PH (ch 22).

SUPPLEMENTARY INFORMATION 2

List of characters excluded from the phylogenetic analyses and the explanation for their exclusion.

From Sterli and de la Fuente (2013), Rabi et al. (2013) and Zhou et al. (2014).

Character numbers and names are as from the most recent update of the character-taxon matrix presented as a Nexus file in Zhou et al. (2014).

Character 8 (Prefrontal E): prefrontal, heavily sculptured with prominences and bosses. JY1 & STF (ch 8, Prefrontal E). Reason for exclusion: uninformative character for Testudines as ingroup.

Character 13 (Parietal B): parietal contact with the pterygoid, epipterygoid, or palatine and Character 14 (Parietal C): length of anterior extension of the lateral braincase wall. Reason for combination: the anterior extension does not allow for the contact between the pterygoid, epipterygoid or palatine, see Character 15 of this study.

Character 16 (Parietal E): processus inferior parietalis forming the posterior margin of the foramen nervi trigemini. Combination: character represented in Character 15 of this study.

Character 18 (Parietal G): parietal, forming part of the foramen stapedio-temporalis. Reason for exclusion: uninformative for Testudines (as ingroup).

Character 28 (Squamosal D): long posterior process protruding beyond condyles occipitalis. Sterli and de la Fuente (2013) indicate that this is a new character, however this is the same as character 24 of Gaffney et al. (2006): Squamosal, Posterior projection. Reason for exclusion: after examination of extant and fossil taxa, we concluded that this character is variable and so we excluded it from this study, however a possible quantification of the size of the posterior projection (out of the scope of this study) could reveal a defined pattern in different lineages with phylogenetic meaning.

Character 37 (Maxilla A): do not contact each other in ventral view. Reason for combination: this is synonymous with vomer-premaxilla contact Character 47 of this study. The contact between both maxillae occurs when the vomer is very small or absent.

Character 38 (Maxilla B): contribution of the palatine to the triturating surface. Reason for combination: this is synonymous with character 41 of this study.

Character 61 (Pterygoid C2): pteygoid-basioccipital contact. Reason for exclusion: this is a character useful to differentiate only two taxa in the whole matrix, becoming autapomorphic. We removed it from this study.

Character 79 (Opisthotic A): processus paroccipitalis. Reason for exclusion: uninformative character for Testudines.

Character 88 (Stapedial artery A): position of the canalis stapedio-temporalis. Reason for exclusion: uninformative character for Testudines.

Charater 93 (Foramen jugulare posterius B): foramen jugulare posterius, bones that separate the foramen from the fenestra postotica. Reason for exclusion: uninformative character, autapomorphic for Lissemys punctata.

Character 95 (Caroticum C). Reason for exclusion: lack of clearly defined character states in recent studies, Sterli and de la Fuente (2013) and Zhou et al. (2014).

Character 96 (Caroticum D) and Character 97 (Caroticum E). Reason for exclusion: both are related to the evolution of the carotid, we redefined two characters (character 103 and 104) to cover all possible states about the internal carotid artery.

Character 101 (Cranial scutes A): presence or absence. This character is synonymous with character 9 of this study.

Characters 106 to 114 (Cranial Scute F, G, H, I, J, K, L, M, N): cranial scutes. Reason for exclusion: uninformative character, autapomorphic inside meiolaniform turtles.

Character 118 (Upper temporal fossa A): Reason for exclusion: character omitted from this study because is uninformative for Testudinata (stem + crown-Testudines).

Character 122 (Carapace C): bony turtle shell. Reason for exclusion: uninformative character for Testudines as ingroup.

Character 139 (Vertebral A): number of vertebral scutes. Reason for exclusion: uninformative character for Testudines as ingroup.

Character 154 (Epiplastron A): the definition presented in Sterli and de la Fuente (2013) (at least in the Nexus file) differs completely from the original definition of Joyce (2007) (Epiplastron A). We reestablished Joyce's (2007) definition of this character, and we consider that the definition presented

by Sterli and de la Fuente (2012) can be combined with character 151 (Entoplastron D). This is character 170 of this study.

Character 157 (Hyo-Hypoplastron A). Reason for exclusion: This is autapomorphic for *Lissemys punctata*.

Characters 209 and 210 (Tail ring B and Tail club A). Reason for exclusion: these are autapomorphic for meiolanids.

Character 211 (Pectoral Girdle A): scapula, horizontal lamina-dorsal process. This is a character that we consider is better defined by three characters, two of which were previously defined by Joyce (2007) (Scapula A and Coracoid A), and a new character related to the anterodorsal ridge of the acromion. The three characters are characters 214, 215 and 216 of this study.

Character 212 (Pectoral Girdle B). Reason for exclusion: uninformative character for Testudines as ingroup.

Characters 234 and 235 (Pes A and Pes B). Reason for exclusion: uninformative character for Testudines as ingroup.

Character 240 (Neural Number): number of neurals. This character has been previously defined in other studies. See character 126 of this study for references.

Character 241 (Plastron Lobe): posterior lobe of plastron. This character is related to the shape of the xiphiplastron and we combined it into character 169 of this study.

Character 243 (Costal Rib) and character 247 (Costal Rib Distal End): we consider this character related to character 134 (Costal C) and include both characters in a redefined character 132 of this study.

Modifications to scoring of previous character-taxon matrix

Characters 240 and 241 (Characters 225 (Ilium B) and 226 (Ilium C), Zhou et al. 2014) *Xinjiangchelys wusu*, *Xjinjianchelys radiplicatoides, Hoplochelys crassa,* and *Anosteira ornata*. Change from "–" to "?".

Character 276 (Character 245 (First vertebral), Zhou et al. 2014) *Palaeochersis talampayensis*. Change from "0" to "?".

Taxa added to the matrix of Zhou et al. (2014)

Brachyopsemys tingitana
Angolachelys mbaxi
Chitracephalus dumonii
Corsochelys haliniches
Nichollsemys bareri
Rhinochelys pulchriceps
Rhinochelys nammourensis
Rhinochelys sp.
Protostega gigas
Archelon ischyros
Bouliachelys suteri
Desmatochelys lowi
Colombiachelys padillai
Mexichelys coahuilaensis
Argillochelys cuneiceps
Argillochelys africana
Tasbacka ouledabdounensis
Eochelone brabantica
Erquelinnesia gosseleti
Pacifichelys spp.
Puppigerus camperi
Allopleuron hoffmanni
Ctneochelys stenoporus
Lepidochelys olivacea
Lepidochelys kempii
Eretmochelys imbricata
Natator depressus
Euclastes acutirostris
Euclastes wielandi
Euclastes platyops
Itilochelys rasstrigin
Calcarichelys gemma
Ocepechelon bouyai
Adocus amtgai
Notoemys zapatocaensis
Alienochelys selloumi
Syllomus aegyptiacus
Tasbacka aldabergeni
Chelosphargis advena
Helochelydra nopcsai
Sandownia harrisi
Hoyasemys jimenezi
Terlinguachelys fischbecki
Lophochelys (natatrix+niobrarae)
Carolinochelys wilsoni
Asleychelys palmeri
Procolpochelys grandaeva

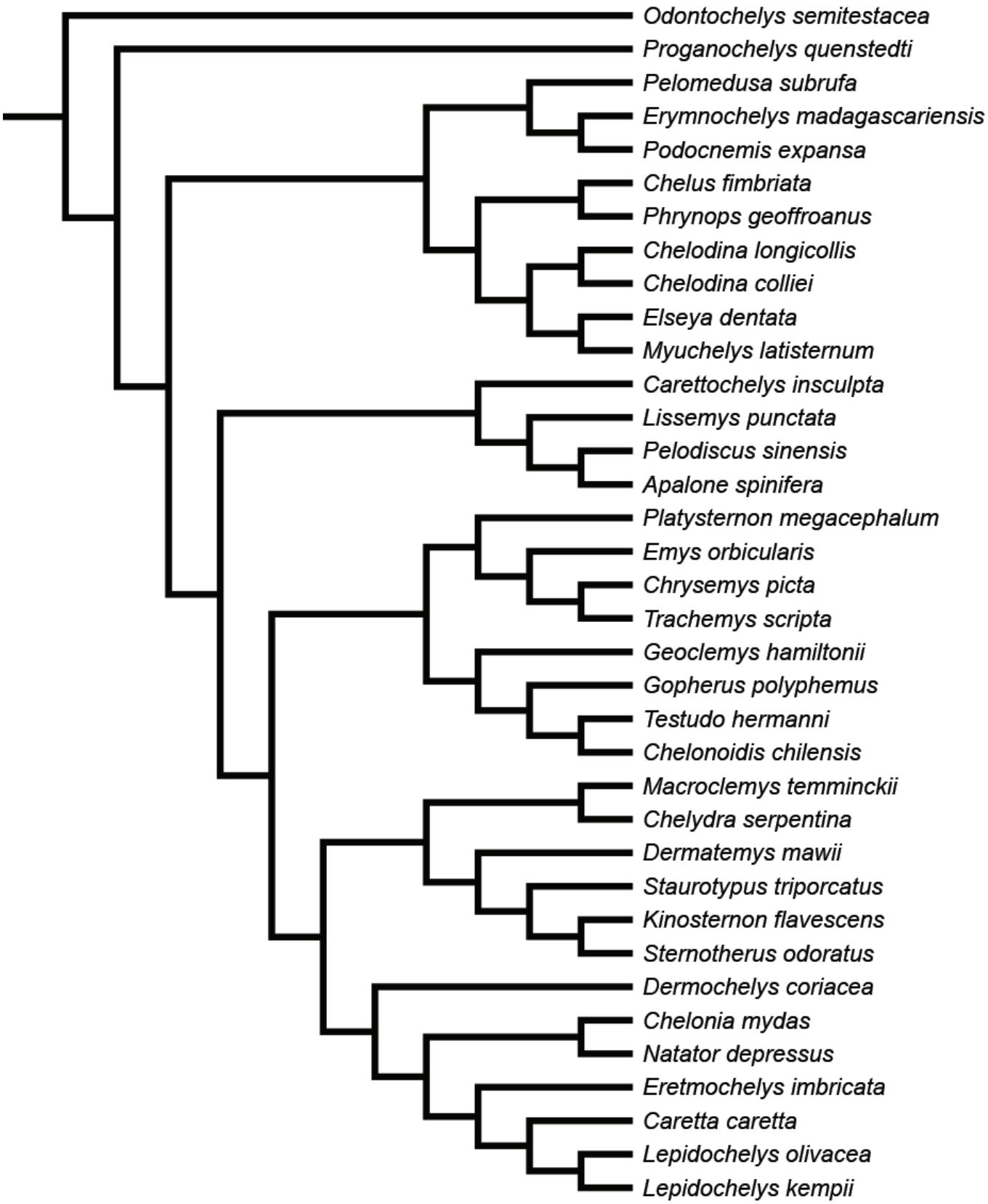

Figure 1S. Backbone constraint tree topology for the extant OTUs used in the phylogenetic analysis (Fig. 11), following the most comprehensive molecular analysis of turtle relationships (Crawford et al. 2015).

Table 1S. List of extant and fossil specimens examined.

EXTANT		
Species	**Collection ID**	**Material**
Caretta caretta	FMNH 1478	Skull-Jaw
Caretta caretta	FMNH 4158	Skull-Jaw
Caretta caretta	FMNH 31020	Skull-Jaw-Postcranial
Caretta caretta	FMNH 34329	Skull-Jaw
Caretta caretta	FMNH 121932	Skull-Jaw-Postcranial
Caretta caretta	MTKD 2392	Skull
Caretta caretta	NCSM 354	Skull-Jaw-Postcranial
Caretta caretta	NCSM 4217	Skull-Jaw
Caretta caretta	NCSM 16007	Skull-Jaw
Caretta caretta	NCSM 30816	Postcranial
Caretta caretta	NCSM 62511	Skull-Jaw
Caretta caretta	NCSM 62546	Skull-Jaw
Caretta caretta	NCSM 62560	Skull-Jaw
Caretta caretta	NCSM 62562	Skull-Jaw
Caretta caretta	NCSM 62563	Skull-Jaw
Caretta caretta	NCSM 79143	Skull-Jaw-Postcranial
Caretta caretta	USNM 31790	Skull-Jaw
Caretta caretta	USNM 317907	Skull-Jaw
Caretta caretta	USNM 317908	Skull-Jaw
Caretta caretta	USNM 317914	Skull-Jaw
Caretta caretta	USNM 317917	Skull-Jaw
Caretta caretta	USNM 317918	Skull-Jaw
Caretta caretta	USNM 347556	Postcranial
Caretta caretta	UCMP 119064	Skull-Jaw
Caretta caretta	SM 32145	Skull-Jaw
Caretta caretta	SM 32143	Skull-Jaw-Postcranial
Chelonia mydas	FMNH 29276	Skull-Jaw
Chelonia mydas	FMNH 51673	Skull-Jaw
Chelonia mydas	FMNH 10449	Postcranial
Chelonia mydas	FMNH 207431	Skull-Jaw
Chelonia mydas	FMNH 212910	Skull-Jaw
Chelonia mydas	NCSM 57902	Skull-Jaw
Chelonia mydas	NCSM 61743	Skull-Jaw
Chelonia mydas	NCSM 62559	Skull-Jaw
Chelonia mydas	NCSM 62567	Skull-Jaw-Postcranial
Chelonia mydas	UCMP 123034	Skull-Jaw
Chelonia mydas	UCMP 132031	Skull-Jaw
Chelonia mydas	USMN 039262	Postcranial

EXTANT		
Species	**Collection ID**	**Material**
Caretta caretta	FMNH 1478	Skull-Jaw
Caretta caretta	FMNH 4158	Skull-Jaw
Caretta caretta	FMNH 31020	Skull-Jaw-Postcranial
Caretta caretta	FMNH 34329	Skull-Jaw
Caretta caretta	FMNH 121932	Skull-Jaw-Postcranial
Caretta caretta	MTKD 2392	Skull
Caretta caretta	NCSM 354	Skull-Jaw-Postcranial
Caretta caretta	NCSM 4217	Skull-Jaw
Caretta caretta	NCSM 16007	Skull-Jaw
Caretta caretta	NCSM 30816	Postcranial
Caretta caretta	NCSM 62511	Skull-Jaw
Caretta caretta	NCSM 62546	Skull-Jaw
Caretta caretta	NCSM 62560	Skull-Jaw
Caretta caretta	NCSM 62562	Skull-Jaw
Caretta caretta	NCSM 62563	Skull-Jaw
Caretta caretta	NCSM 79143	Skull-Jaw-Postcranial
Caretta caretta	USNM 31790	Skull-Jaw
Caretta caretta	USNM 317907	Skull-Jaw
Caretta caretta	USNM 317908	Skull-Jaw
Caretta caretta	USNM 317914	Skull-Jaw
Caretta caretta	USNM 317917	Skull-Jaw
Caretta caretta	USNM 317918	Skull-Jaw
Caretta caretta	USNM 347556	Postcranial
Caretta caretta	UCMP 119064	Skull-Jaw
Caretta caretta	SM 32145	Skull-Jaw
Caretta caretta	SM 32143	Skull-Jaw-Postcranial
Chelonia mydas	FMNH 29276	Skull-Jaw
Chelonia mydas	FMNH 51673	Skull-Jaw
Chelonia mydas	FMNH 10449	Postcranial
Chelonia mydas	FMNH 207431	Skull-Jaw
Chelonia mydas	FMNH 212910	Skull-Jaw
Chelonia mydas	NCSM 57902	Skull-Jaw
Chelonia mydas	NCSM 61743	Skull-Jaw
Chelonia mydas	NCSM 62559	Skull-Jaw
Chelonia mydas	NCSM 62567	Skull-Jaw-Postcranial
Chelonia mydas	UCMP 123034	Skull-Jaw
Chelonia mydas	UCMP 132031	Skull-Jaw
Chelonia mydas	USMN 039262	Postcranial
Chelonia mydas	USMN 117363	Head

EXTANT		
Species	**Collection ID**	**Material**
Eretmochelys imbricata	USNM 231696	Skull-Jaw
Eretmochelys imbricata	USNM 237710	Skull-Jaw-Postcranial
Eretmochelys imbricata	USNM 267026	Postcranial
Eretmochelys imbricata	USNM 279317	Complete specimen
Eretmochelys imbricata	USNM 237699	Skull-Jaw-Postcranial
Lepidochelys kempii	FMNH 275847	Skull-Jaw-Postcranial
Lepidochelys kempii	FMNH 31334	Skull-Jaw-Postcranial
Lepidochelys kempii	NCSM 21164	Complete skeleton
Lepidochelys kempii	NCSM 62564	Skull-Jaw-Postcranial
Lepidochelys kempii	NCSM 62565	Skull-Jaw
Lepidochelys kempii	NCSM 67080	Postcranial
Lepidochelys kempii	USNM 220818	Skull-Jaw-Postcranial
Lepidochelys kempii	USNM 220819	Skull-Jaw-Postcranial
Lepidochelys kempii	USNM 227688	Skull-Jaw-Postcranial
Lepidochelys kempii	USNM 227691	Skull-Jaw
Lepidochelys kempii	USNM 235603	Skull-Jaw
Lepidochelys kempii	USNM 291940	Skull-Jaw
Lepidochelys kempii	USNM 292989	Skull-Jaw
Lepidochelys kempii	USNM 308591	Postcranial
Lepidochelys olivacea	MTKD 11175	Skull
Lepidochelys olivacea	USNM 095416	Skull-Jaw
Lepidochelys olivacea	USNM 214142	Skull-Jaw-Postcranial
Lepidochelys olivacea	USNM 300031	Skull-Jaw-Postcranial
Lepidochelys olivacea	USNM 300057	Skull-Jaw
Lepidochelys olivacea	USNM 300064	Skull-Jaw
Dermochelys coriacea	UCMP 130642	Skull-Jaw
Dermochelys coriacea	USNM 062754	Postcranial
Dermochelys coriacea	USNM 063491	Postcranial
Dermochelys coriacea	USNM 220843	Postcranial
Dermochelys coriacea	USNM 228844	Skull-Jaw
Dermochelys coriacea	USNM 243396	Skull-Jaw
Dermochelys coriacea	USNM 243397	Skull-Jaw
Dermochelys coriacea	USNM 243401	Skull-Jaw
Dermochelys coriacea	USNM 243402	Skull-Jaw
Dermochelys coriacea	USNM 317614	Skull-Jaw
Dermochelys coriacea	USNM 317616	Skull-Jaw
Dermochelys coriacea	USNM 317618	Skull-Jaw
Natator depresus	SM 32411	Skull-Jaw-Postcranial

FOSSILS		
Species	**Collection ID**	**Material**
Archelon ischyros	NMW Vienna specimen	Complete skeleton
Protostega gigas	USNM 11652	Skull
Toxochelys latiremis	MCZ 1046	Skull
Rhinochelys sp. (HIGH RESOLUTION IMAGES)	SM B55775	Skull
Rhinochelys sp. (HIGH RESOLUTION IMAGES)	SM B55792	Skull
Demastochelys padillai	FCG–CBP 01	Nearly complete skeleton
Demastochelys padillai	FCG–CBP 40	Skull and jaw
Demastochelys padillai	FCG–CBP 13	Skull and jaw
Demastochelys padillai	FCG–CBP 39	Skull and jaw
Demastochelys padillai	UCMP 38346	Skull and jaw
Demastochelys padillai	UCMP 38345A	Partial carapace
Demastochelys padillai	UCMP 38345B	Posterior portion carapace

Institutional abbreviations

FCG–CBP, Fundación Colombiana de Geobiología, Centro de Investigaciones Paleontológicas, Villa de Leyva, Colombia
FMNH (Florida Museum of Natural History, Herpetology collection, Gainesville, Florida, USA)
MCZ (Museum of Comparative Zoology, Harvard University, Cambridge, Massachusetts, USA)
MTKD (Senckenberg Natural History Collections, Dresden, Germany)
NCSM (North Carolina Science Museum, Raleigh, USA)
NMW (Naturhistoriches Museum Wien, Viena, Austria)
SM (Sedgewick Museum, Cambridge, UK)
UCMP (University of California Museum of Paleontology, herpetology collection, Berkeley, USA)
USNM-SM (Smithsonian National Museum of Natural History, herpetology collection, Washington, USA)